Transportation Research Part C 140 (2022) 103699

Contents lists available at ScienceDirect

Transportation Research Part C

journal homepage: www.elsevier.com/locate/trc

Adaptive cell-based evacuation systems for leader-follower crowd evacuation

Miguel A. Lopez-Carmona *, Alvaro Paricio Garcia

Universidad de Alcala, Escuela Politecnica Superior, Departamento de Automatica, Campus Externo de la Universidad de Alcala, Alcala de Henares, Madrid, Spain

ARTICLE INFO

Keywords:
Crowd evacuation
Leader-based evacuation
Exit-choice decision-making
Simulation–optimization
Cell-based evacuation
Evacuation safety

ABSTRACT

The challenge of controlling crowd movement at large events expands not only to the realm of emergency evacuations but also to improving non-critical conditions related to operational efficiency and comfort. In both cases, it becomes necessary to develop adaptive crowd motion control systems. In particular, adaptive cell-based crowd evacuation systems dynamically generate exit-choice recommendations favoring a coordinated group dynamic that improves safety and evacuation time. We investigate the viability of using this mechanism to develop a "leader-follower" evacuation system in which a trained evacuation staff guides evacuees safely to the exit gates. To validate the proposal, we use a simulation–optimization framework integrating microscopic simulation. Evacuees' behavior has been modeled using a three-layered architecture that includes eligibility, exit-choice changing, and exit-choice models, calibrated with hypothetical-choice experiments. As a significant contribution of this work, the proposed behavior models capture the influence of leaders on evacuees, which is translated into exit-choice decisions and the adaptation of speed. This influence can be easily modulated to evaluate the evacuation efficiency under different evacuation scenarios and evacuees' behavior profiles. When measuring the efficiency of the evacuation processes, particular attention has been paid to safety by using pedestrian Macroscopic Fundamental Diagrams (p-MFD), which model the crowd movement dynamics from a macroscopic perspective. The spatiotemporal view of the evacuation performance in the form of crowd-pressure vs. density values allowed us to evaluate and compare safety in different evacuation scenarios reasonably and consistently. Experimental results confirm the viability of using adaptive cell-based crowd evacuation systems as a guidance tool to be used by evacuation staff to guide evacuees. Interestingly, we found that evacuation staff motion speed plays a crucial role in balancing egress time and safety. Thus, it is expected that by instructing evacuation staff to move at a predefined speed, we can reach the desired balance between evacuation time, accident probability, and comfort.

1. Introduction

Research on crowd evacuations has paid much attention to emergency scenarios (Helbing and Mukerji, 2012). However, congestion management and operational inefficiency in the use of infrastructures remain an issue (Murakami et al., 2020). Thus, whether the objective is to manage evacuation emergencies or improve non-critical conditions related to comfort, reduce contacts between people, or operational efficiency, research in adaptive crowd evacuation systems takes on a very relevant role. The objective is to control crowd movements in real-time to ensure no dangerous situation occurs, guaranteeing reasonable egress times.

* Corresponding author.
E-mail addresses: miguelangel.lopez@uah.es (M.A. Lopez-Carmona), alvaro.paricio@uah.es (A. Paricio Garcia).

https://doi.org/10.1016/j.trc.2022.103699
Received 22 July 2021; Received in revised form 4 January 2022; Accepted 17 April 2022
Available online 4 May 2022

Adaptive crowd evacuation management has a clear connection with available technologies. Modern crowd detection technologies (Jacques et al., 2010; Kaiser et al., 2018), positioning systems (Nguyen-Huu et al., 2017), pedestrian tracking systems (Johansson et al., 2008; Brunetti et al., 2018) and high-performance computing should be translated into the development of real-time crowd evacuation systems (Kok et al., 2016; Haghani, 2020a), taking advantage of all the accumulated know-how about crowd dynamics (Helbing and Molnár, 1995; Zhang et al., 2012). Efficient real-time coordination of evacuees (Bi and Gelenbe, 2019) can be achieved by deploying guidance systems that dynamically inform to pedestrians about exits (Lopez-Carmona and Paricio Garcia, 2021), the paths (Wang et al., 2015), speed (Truong et al., 2019), and the evacuation start time (Abdelghany et al., 2014; Murakami et al., 2020).

The performance of crowd evacuations can be strongly affected by individual exit-choice decisions (Kinateder et al., 2018; Chen et al., 2018; Haghani and Sarvi, 2019b; Feliciani et al., 2020). Therefore, behavioral modification methods through optimal active instructions have the potential to effectively make people be part of the evacuation solution, as stated in the systematic review of optimization methods for pedestrian evacuations in Haghani (2020b), which presents the "behavioral optimization" concept and its relevance in optimizing crowd evacuations.

Research efforts in real-time guidance for crowd evacuations have proposed mechanisms for providing pedestrians with dynamic exit-choice information. Several studies have focused on providing optimal exit-choice information using optimal static plans obtained through simulation–optimization methods (Abdelghany et al., 2014; Guo, 2018). However, in this paper, we are interested in adaptive strategies since, in realistic scenarios, the environment dynamics may change over time in unpredictable ways (Zhong et al., 2016).

Crowd evacuation management based on dynamic information about the exit-choice or speed is challenging, not only because of the potential algorithmic complexity in the design of mechanisms but also because of the usability of the system. The information provided by the system must be easy to understand and translate into individual actions if these systems are to work in real-world scenarios (Ferscha and Zia, 2010). Cell-based crowd evacuation systems emerge as reliable candidates to support coordinated pedestrian dynamics using existing technologies (Zhong et al., 2016; Guo, 2018; Lopez-Carmona and Paricio-Garcia, 2020; Lopez-Carmona and Paricio Garcia, 2021). In these systems, pedestrians receive guidance information dynamically depending on their position in a cell-based pedestrian positioning infrastructure. Though guidance information has been typically restricted to exit-choice recommendations, it can be extended, for instance, to trajectory or speed recommendations.

Within the "behavioral optimization" research line defined in Haghani (2020b), our previous research (Lopez-Carmona and Paricio Garcia, 2021) proposed an adaptive guidance system (Cell-based Crowd Evacuation, CellEVAC) that provides optimal exit-choice instructions through wearable devices. CellEVAC implements a heuristic function that integrates influential factors on exit-choice decision-making, which is optimized using a simulation–optimization methodology. This function works as a controller to generate the exit-choice indications. Our system exhibited better overall performance than previous approaches based on Cartesian Genetic Programming (Zhong et al., 2016,b).

As an extension of Lopez-Carmona and Paricio Garcia (2021), in Lopez-Carmona and Paricio-Garcia (2020) we proposed a system architecture for CellEVAC based on the use of light-emitting diode (LED) wristbands, a controller node, and a network of Radio Frequency Identification (RFID) devices. We aimed to study the sensitivity of evacuation time and safety to uncertainty in the positioning system.

An important aspect to consider when analyzing the efficiency of this type of systems is how the compliance rate influences evacuation efficiency (Lopez-Carmona and Paricio Garcia, 2021). How many evacuees are to use the system and behave when receiving instructions. In the existing literature on cell-based evacuation systems, typically, evacuation scenarios assume that the entire population is a system user (Abdelghany et al., 2014; Zhong et al., 2016). Our proposal in Lopez-Carmona and Paricio Garcia (2021) evaluated scenarios with two subpopulations of evacuees. One group of evacuees with wearable devices committed to following the instructions, and another group that does not heed exit recommendations, whose behavior is modeled using a simple exit choice model that does not capture the influence of adjacent pedestrians' wearing wristbands. In this paper, our proposal is use CellEVAC as a leader-follower guidance system in which trained evacuation personnel ("leaders" hereafter), wearing the wristbands, guide the rest of pedestrians ("followers" hereafter). Thus, the extension of existing behavioral models to capture the influence of leader agents is mandatory.

In Zhou et al. (2019a), a survey on guided crowd evacuation analyses existing research on crowd evacuation with leaders. Most research has been focused on proposing microscopic models to simulate guided crowd dynamics and investigate the effect of leaders on evacuation efficiency (Lu et al., 2017; Mao et al., 2019; Xie et al., 2021). The existing literature also includes proposals based on optimal control that aim at minimizing constraints imposed on the system, such as trajectory optimization and evacuation time minimization (Tianhe and Ziheng, 2018). The limitation of these works is that they are not thought to be applied to practical scenarios but to evaluate optimal behaviors from a theoretical perspective. A similar approach can be found in Zhang and Jia (2021), which proposes to obtain an optimal guidance strategy based on exit selection and leaders' location plan using a cell transmission model. However, the guidance strategy is not adaptive so that the optimal values are obtained through a simulation–optimization process and remain unchanged during the evacuation process. Also, in Zhou et al. (2019b), a social force model is extended to model the dynamics of leaders and followers. Authors formulate an optimization problem that determines the initial location of leaders as well as the optimal evacuation routes for the evacuation leaders. To the best of our knowledge, there is a gap in the existing literature regarding adaptive leader–follower-based crowd evacuation systems applied to realistic evacuation scenarios.

Our central hypothesis is that a cell-based guidance system including exit recommendations, in which a reduced number of leaders receive instructions from the evacuation system through the wristbands, trained to move at a predefined speed, and with

an informed population of the existence of leaders, can facilitate efficient and safe evacuation processes with existing technologies and at a reasonable cost.

We are interested in evaluating the benefits of using the adaptive cell-based evacuation paradigm as a leader-based guidance system. Consequently, another central question of our study concerns modeling follower pedestrian behavior to assess the efficiency of the guidance system. Which could be a valid alternative to model the imitation or following behavior? We are also interested in applying a consistent safety metric, considering a macroscopic safety measurement covering the whole evacuation area.

With the purposes mentioned, an adaptive leader-based crowd guidance system is proposed. Colors (indications) corresponding to an exit gate are dynamically displayed in the leaders' LED wristbands depending on their cell position. The system's kernel is a heuristic function that dynamically allocates exit gates depending on several sensed environmental factors, optimized using a simulation–optimization method attending to local congestion and evacuation time goals. The heuristic function embodies influential factors that would operate on individual exit-choice decision-making. These factors include the (i) flow of pedestrians to exit gates, (ii) congestion at exits, (iii) distance, and (iv) inertia to maintaining the previous recommendations. A reduced number of trained evacuation staff members (leaders) are expected to wear the LED wristbands and follow the indications provided by the system, approaching the exit gates at a predefined target average speed.

To model evacuees (followers) behavior, we use the three-layered exit-choice behavior model architecture proposed by Haghani and Sarvi (2019b), with eligibility, exit-choice changing, and exit-choice modules, which has been extended to capture the influence of leaders on evacuees in terms of exit-choice and speed. These modules are implemented with a discrete-choice modeling framework based on random utility theory and calibrated with already existing hypothetical-choice experiments (Haghani et al., 2014, 2016; Haghani and Sarvi, 2017).

The type of hazard that causes the need to evacuate plays a main role in the viability of an evacuation system. Our proposal is expected to be valid in two general evacuation scenarios. Firstly, in non-emergency evacuation scenarios, where the goal is to improve operational efficiency by trading-off evacuation time and safety (e.g., in music concert tours where operational efficiency is a must). Secondly, in emergency evacuation scenarios where the hazard does not disproportionately influence evacuation staff or the evacuee's urgency levels. The three-layered proposed model for follower behavior is calibrated for real scenarios in which the direct influence of the hazard on pedestrian behavior is not physical. So, our proposal would not be valid in general, for instance, for explosions within the evacuation area. However, it would be valid for bomb threats or any other kind of external threat.

In the validation of our proposal, we conduct extensive simulations and measure the evacuation efficiency in three dimensions, egress time, safety, and the number of decision changes. We pay particular attention to crowd safety, measured from a macroscopic perspective using pedestrian Macroscopic Fundamental Diagrams as proposed in Saberi and Mahmassani (2014), Hoogendoorn et al. (2018), using crowd-pressure vs. density values, (Helbing and Molnár, 1995; Feliciani and Nishinari, 2018) and propose a threshold-based method to compare safety in different evacuation scenarios.

This study contributes to the growing literature on interventional approaches that seek to improve evacuation efficiency rather than predict or describe evacuations. The paper makes several contributions to the literature on optimization approaches based on behavioral modification, training, and active instructions, which is gaining increasing attention as a promising method in both effectiveness and practicality (Haghani, 2020b). More specifically, the paper fills a gap in the existing literature about the practicality of leader–follower-based crowd evacuation systems.

First, this study adds to the leader-following crowd evacuation research, providing insights on the first use of cell-based evacuation systems to manage the evacuation staff's motion adaptively. Second, our paper contributes with a comprehensive and calibrated behavior model based on three layers, which is distinct from similar studies by considering the influence of the evacuation staff in terms of exit-choice and speed. This proposal of a three-layered behavior model for follower pedestrians is also an important contribution from an architectural perspective, from which different leader-following patterns can be easily formulated and tested. Third, in contrast to most existing research on interventional approaches aiming to optimize egress time, we also consider safety by evaluating crowd motion from a macroscopic perspective, which has allowed us to augment our understanding of the balance between egress time and safety in leader-follower evacuations. Fourth, this study helps provide a better understanding of how the heterogeneity of the population of followers influences evacuation performance. Finally, this study provides evidence that the proposed modeling architecture can fit different guidance system modeling alternatives.

The rest of the paper is organized as follows. Section 2 presents the evacuation scenario, and the CellEVAC system, including the control logic. Section 3 outlines our modeling framework for evacuees (followers), which includes the conceptualization of exit-choice models, eligibility mechanism, exit-choice decision changing and exit-choice decision, and mechanism for the choice of speed. The evacuation efficiency metrics are outlined in Section 4, mainly focused on describing the measurement of congestion and safety. Section 5 presents the experimental evaluation, based on microscopic simulation analyses. The last two sections provide the discussion, concluding comments and possible research extensions.

2. Evacuation scenario and CellEVAC evacuation system

Located in Madrid (Spain), Madrid Arena is an indoor arena with a capacity of 10,248 spectators. In 2012, a stampede at a Halloween party resulted in the death of five girls due to the excess of capacity, the errors in the indications of the evacuation staff and police, and the absence of a guidance system to help evacuees (BBC news, 2012). In this paper, we studied the evacuation of the ground floor with the retractable bleachers removed and a maximum capacity of 3,400 spectators (see Fig. 8 in the experimental section).

2.1. CellEVAC evacuation system

In Lopez-Carmona and Paricio Garcia (2021), we presented an adaptive cell-based crowd evacuation system (CellEVAC) that searches for the optimal control function through meta-heuristic optimization methodology. The cell-based system provides optimal exit-choice individual recommendations through color codes to all the pedestrians in the facility. Also, we investigated in Lopez-Carmona and Paricio-Garcia (2020) how to use existing location-aware technologies and wearable devices in the real deployment of CellEVAC and quantitatively studied the sensitivity of evacuation time and safety to uncertainty in positioning systems. Our proposal is to use CellEVAC to guide leader agents during evacuation. In the following, we briefly recall the architecture and control logic that builds the CellEVAC system.

We divide the ground floor into 42 regular hexagonal cells of $9m^2$ and $6m$ width (Fig. 8), which provide a reasonable balance between control capability, wireless coverage, and computational efficiency. Light-emitting diode (LED) wristbands, widely used at various event types, from live acts at arenas to sports matches, and corporate events, provide real-time exit gate indications to pedestrians through the color codes.

The system architecture consists of three subsystems:

1. Monitoring and control logic subsystem (Controller node).
2. Active RFID cell node network (Positioning system).
3. Radio-controlled LED wristbands, with an RFID Reader and radio-frequency (RF) communication capabilities.

The pedestrian flow estimation block in the controller periodically estimates pedestrian density. This block is built on commercially available pedestrian counting technology (Kurkcu and Ozbay, 2017; Akhter et al., 2019; Lesani et al., 2020; Ilyas et al., 2020). Pedestrian flow estimation feeds the control logic block that periodically computes the optimal allocation of colors to cells. An RF transmitter broadcasts messages every four seconds containing the 42 tuples $\{Cell, Color\}$ that assign a color to each cell.

Cell nodes are equipped with active RFID tags (Chen et al., 2019) that periodically broadcasts its ID (active RFID beacon (Correa et al., 2017)). The wristbands embed an RFID reader that selects the message ID with the highest Received Signal Strength Indicator (RSSI) to estimate the cell location (Alvarez Lopez et al., 2017). The RF Receiver in the wristband periodically evaluates the broadcast messages with the tuples $Cell, Color$ from the controller node. The wristband lights up with the corresponding exit gate color by matching the selected cell ID and cell-color tuples.

2.2. Control logic of CellEVAC for leader-based guidance

The control logic module in the CellEVAC system architecture focuses on optimally allocating colors to cells, an adaptive process that responds to changing environmental conditions monitored by the pedestrian flow estimation block. The control logic module is implemented as a heuristic function based on a behavioral optimization approach proposed in Lopez-Carmona and Paricio Garcia (2021). However, in this work, we propose to use a two-step methodology to find the parameters that define the heuristic function. Also, the parameters have been defined and normalized differently.

Inspired by the pedestrians' exit-choice decision modeling based on the Multinomial Logit Model (MLM) (Ortúzar and Willumsen, 2011; Duives and Mahmassani, 2012; Haghani et al., 2016), the heuristic used is a scoring function V_{cj} for cell c and exit gate j, which is given by:

$$V_{cj} = \beta_D \times DIST_{cj} + \beta_C \times CONG_j + \beta_F \times FLTOEX_{cj} + \\ +\beta_{In}(t) \times Inertia_{cj} \tag{1}$$

The exit gate/color selected for cell c at time t will be the exit gate j that gives the highest score value, being the control mechanism deterministic, in contrast to the pedestrian behavior modeling, which is probabilistic. Thus, in contrast to the three-layered model proposed in this paper for pedestrian behavior (Section 3), the CellEVAC mechanism for generating exit-choice indications only includes one decision-making layer.

In Eq. (1), $DIST_{cj}$ represents the distance from cell c to exit j, normalized in the range of 0–1. $CONG_j$ represents the congestion at each exit gate j defined as the pedestrian density value normalized by the maximum density value found at the different exit gates. The third attribute is $FLOTEX_{cj}$, which measures the pedestrian flow to exit gate j, relative to the highest flow measured from cell c. The parameters β_D, β_C and β_F weigh the relative importance of each attribute, defined as constant values for all V_{cj}. These parameters are expected to take negative values if the selection of exit gates is favored by shorter distances and less congestion at exits and pedestrian flows.

The fourth attribute is the $Inertia$ value, which models how the controller is likely to revise the previous exit gate allocations. The main objective of this parameter is to modulate the changing ratio and avoid the flip-flop effect. This attribute is defined as a binary categorical 0–1 value that equals 1 if the previous exit gate of cell c is j, and is 0 otherwise. For example, for a given cell c let us assume that the previous allocation is exit gate k. When calculating the new V_{cj} values for cell c, $Inertia_{cj} = 1$ if $j == k$ and $Inertia_{cj} = 0$ otherwise. In a general context, $\beta_{In}(t)$ will take positive values to modulate the probability of selecting the current exit gate. Note that with negative values, we would be modulating the probability of avoiding the current exit gate. In contrast to the other parameters, the parameter modulating the $Inertia$ attribute has been defined as time-dependent as follows:

$$\beta_{In}(t) = \beta_{In} \times \left(1 - \frac{peds(t)}{peds(t=0)}\right) \tag{2}$$

Table 1
Optimal configuration of the parameters of the CellEVAC heuristic function.

	β_D	β_C	β_F
CellEVAC	−7.709	−2.815	−2.49

According to Eq. (2), the parameter $\beta_{In}(t)$ tends to β_{In} as evacuation progresses. The frequency of the changes can be modulated using the parameter β_{In}, for an update cycle of 4 s which is kept constant.

2.3. Simulation–optimization for configuring the control logic

To configure the parameters of the heuristic function V_{cj}, we first performed simulation–optimization experiments to find values for coefficients β_D, β_C, and β_F that minimize the sum of evacuation time (measured in seconds) and variance of the cumulative pedestrian densities (in peds/m^2) at the exit gates (Eq. (3)). By including the variance of cumulative densities, our objective was to search for a control logic that would balance the pedestrian flows at the exits. Note that the *Inertia* parameter is excluded from the simulation–optimization process.

$$\min(evactime + \text{Var}\{cumulativeDensity_{j=1\ldots N}\}) \tag{3}$$

The simulation–optimization process adopts the Tabu-Search algorithm (TS) (Glover, 1997), using the simulation–optimization framework that we developed in Lopez-Carmona and Paricio Garcia (2021). Each microscopic crowd evacuation simulation guides the search by evaluating the fitness (Eq. (3)) of the solutions generated by the TS algorithm (e.g., the different tuples β_D, β_C and β_F). The different combinations of parameters of the CellEVAC heuristic function (β_D, β_C and β_F) are the "CellEVAC heuristic function candidates". The simulation results (evacuation time and variance of cumulative density at exit gates) from each evacuation simulation for a given tuple of parameters guide the optimization process.

In Haghani and Sarvi (2019a), different compositions of exit choice behaviors in a human crowd are tested to investigate the influence of the penetration rate of optimal choice behavior in evacuation efficiency. For a penetration rate of optimal behavior of 50% and above, the benefits in the evacuation efficiency become marginal. Intuitively, to configure the evacuation scenario to perform the simulation–optimization process, the composition should include a population following the desired behavior of at least 50%. Thus, in our simulation–optimization process, we have assumed a population of 3400 pedestrians, and that all use the CellEVAC system.

There does not exist a unique possibility of combining simulation and optimization (Figueira and Almada-Lobo, 2014). One of the factors that influence the efficiency of the search process of an optimal solution is the search scheme that relates realizations/simulations (replicas) and solutions. If we apply a 1–1 scheme, and the stochasticity of realizations is high, the search process may become myopic. Our strategy is to apply a [3–10] to 1 scheme, which estimates for each new replica and the previous replicas of a given solution the average value of all the results obtained, and the corresponding confidence interval. By increasing the number of replicas, the confidence interval is expected to be progressively reduced. The simulations for a given solution end when the confidence interval is below a predefined error percentage around the average value, or when the maximum number of replicas is reached. Up to our knowledge, there is no general method to define the minimum and the maximum number of replicas. Usually, this is made by observing the convergence of the optimization process. The range [3–10], with a confidence interval of 90%, 5% of error as threshold, and 200 iterations (heuristic function candidates) provides a good convergence. Thus, for 200 iterations, there will be 200 heuristic function candidates and between $200 \times 3 = 600$ and $200 \times 10 = 2000$ simulations.

The resulting configuration from the optimization process is shown in Table 1. As expected, all the parameters took negative values, with an influence of the distance parameter that doubled the influence of congestion and pedestrian flows to exits.

Finally, in the second step for configuring the control logic, using the optimal configuration of parameters β_D, β_C and β_F, we varied manually β_{In}. We found that $\beta_{In} = 3$ induced a reasonable changing ratio with good performance results. Though it would have been possible to include the $Inertia$ in the optimization process, we found it more practical to manually modulate the changing ratio to the desired level to keep the exit indications' changing ratio to reasonable values.

3. Pedestrian behavior modeling

The knowledge of the influence factors on evacuees' behavior is crucial when designing evacuation systems. To capture the influence of these factors researchers rely on simulated or virtual environments (Bode and Codling, 2013; Bode et al., 2014, 2015), and decision-making models calibrated with revealed and stated preferences (Haghani et al., 2014), in which exit-choice strategies play a main role (Hoogendoorn and Bovy, 2004; Kinateder et al., 2018; Chen et al., 2018; Duives and Mahmassani, 2012).

In our evacuation scenario, two different forms of pedestrian behavior can be broadly distinguished. The behavior of the CellEVAC leaders who wear LED wristbands and choose the exits indicated by the CellEVAC system, and that of pedestrians who do not wear LED wristbands, and attend to external factors in the decision-making processes for the choice of exit. The movement during evacuation simulations is governed by the microscopic SFM model and exit-choice in both behavior models.

CellEVAC leaders strictly follow the exit gate recommendations of the CellEVAC system. Therefore, the leaders located in a cell c that recommends exit gate k, will choose exit gate k as the destination. We assumed that leaders walked during the evacuation at a recommended average velocity to guide other pedestrians.

In the following, this section focuses on developing the exit-choice behavior model for pedestrians who do not wear LED wristbands (followers). This model is implemented in the Pedestrians' exit-choice/Pedestrians' MLM exit-choice module of the simulation–optimization framework.

3.1. Followers' exit-choice model conceptualization

The first task we tackled was to choose a discrete-choice modeling framework. Our choice was to use the most widely used theoretical framework, based on random utility theory (Antonini et al., 2006; Ben-Akiva and Bierlaire, 1999; Press, 1985; Ortúzar and Willumsen, 2011), which is the discrete choice model logit (Luce, 1958; Train, 2009; Ortúzar and Willumsen, 2011). Its popularity relies upon the fact that the choice probability formula takes a closed-form and is easily interpretable.

This theoretical framework states that:

1. Pedestrians belong to a homogeneous population P.
2. There is a set $\mathbf{E} = \{E_1, \ldots, E_j, \ldots, E_N\}$ of alternatives and a set $\mathbf{X}$ of vectors of attributes of the pedestrians and their alternatives. A given pedestrian p is provided with a particular set of attributes $\mathbf{x} \in \mathbf{X}$ and will face a choice set $\mathbf{E}(p) \in \mathbf{E}$.
3. Each option $E_j \in \mathbf{E}$ has associated a utility U_{pj} for pedestrian p. It is assumed that U_{pj} can be represented by two components:
   (a) V_{pj} which is a function of the measured attributes $\mathbf{x}$; and
   (b) a random part ε_{pj} which reflects the idiosyncrasies of each individual and any observational error.

   Thus, we may postulate that:

   $$U_{pj} = V_{pj} + \varepsilon_{pj}$$

   $\mathbf{V}$ carries the subscript p because it is a function of the attributes $\mathbf{x}$ and this may vary between pedestrians. It can be assumed that the residuals ε are random variables with mean 0 and a certain probability distribution to be specified. A typical expression for $\mathbf{V}$ is:

   $$V_{pj} = \sum_k \beta_{jk} x_{pjk}$$

   where the parameters (coefficients) β may vary across alternatives but are assumed to be constant for all individuals.
4. The pedestrian p selects the maximum-utility alternative E_j if and only if:

   $$V_{pj} - V_{pi} \geqslant \varepsilon_{pi} - \varepsilon_{pj}$$

   Thus, the probability of choosing E_j is:

   $$P_{pj} = \text{Prob}\{\varepsilon_{pi} \leqslant \varepsilon_{pj} + (V_{pj} - V_{qi}), \forall E_i \in E(p)\}$$

   and as the joint distribution of the residuals is not known, different model forms may be generated.

The logit model is obtained by assuming that the error terms are independently, identically distributed (IID) extreme values. The distribution is also called Gumbel and Extreme Value Type I. With this assumption, the choice probabilities of a given option j by pedestrian p are:

$$P_{pj} = \frac{\exp(V_{pj})}{\sum_{E_i \in E(p)} \exp(V_{pi})} \tag{4}$$

The model is called the Multinomial Logit Model (MLM) when more than two options are available. In decision-making processes with only two options, the formula is reduced to a binary logit formula, in which the coefficients of the utility function of one of the two alternatives are set to zero to meet the identification requirements of the model.

Once the discrete-choice modeling framework was chosen, the next step was to decide how to formalize the adaptive exit-choice processes. Studies have paid a great deal of attention to modeling directional decision making (Duives and Mahmassani, 2012; Haghani et al., 2014; Bode et al., 2014, 2015; Haghani et al., 2016; Haghani and Sarvi, 2017, 2018), in which the decision-making process is based exclusively on an evaluation of the attributes of each exit gate and the individual characteristics of the pedestrian, this being a dynamic and periodic single-stage process. However, it is well known that strategy adaptation is a multi-dimensional process that can be observed concerning several aspects of pedestrians' behavior. In Haghani and Sarvi (2019b) identify at least four different dimensions in strategy adaptation: local navigation (Antonini et al., 2006), global pathfinding (Kneidl et al., 2013), reaction decisions (Bode and Codling, 2019), exit direction choices (Ehtamo et al., 2010; Duives and Mahmassani, 2012; Bode and Codling, 2013; Haghani et al., 2015; Kinateder et al., 2018), and choice of speed (Fridolf et al., 2013). Moreover, it is crucial for modeling purposes to capture how during evacuations, humans adjust their previous choices in response to the changing environment to improve their strategies, which implies considering the historical evolution and current state of the decision-making process.

In Haghani and Sarvi (2019b), a discrete choice model is proposed that incorporates the fundamental factors that influence the tendency to revise previous exit decisions. The exit choice decision-making process is implemented with a three-phase iterative

process. The first phase includes an initial eligibility mechanism, determining if pedestrians can change their previous exit choice. This phase incorporates those factors that make it possible to determine whether exit-choice changing is physically unfeasible or unnecessary. For pedestrians that can change their decisions, in the second phase, a Binary Logit Model is used to decide on changing of exit gate by evaluating environmental and individual factors. The last phase makes the final exit-choice using a Multinomial Logit Model, calibrated with real laboratory simulation data.

Later, in Lopez-Carmona and Paricio Garcia (2021), we took a different approach to model decision-making by including a time-dependent inertia parameter in the exit choice formula to reinforce the previous exit-choice decisions to a given degree. This strategy allowed us to simplify the formulation and speed up behavioral optimization processes. However, we did not include any eligibility mechanism, and the MLM was not calibrated because our goal was to find optimal strategies. Although it would have been possible to use a two-phase process with an eligibility mechanism and an exit-choice model including an inertia parameter, in this work, it was decided to apply Haghani's structure of three stages for neutrality and calibration reasons.

The final step in the followers' exit-choice model conceptualization was to identify the influential factors that explain pedestrians' decision-making (Duives and Mahmassani, 2012; Lovreglio et al., 2014; Kinateder et al., 2018). The first criterion in choosing the attributes of the model was their relevance reported by the literature. The second criterion was the number of attributes to include, considering that a small number of attributes benefits model calibration and interpretation (Haghani and Sarvi, 2019b). The third consideration was the structural decision of defining a three-layered model, including the eligibility, exit-choice changing, and directional decision-making. The final consideration was the necessity of modeling the influence of leaders on pedestrians.

Thus, we assumed that exit-choice changing is motivated by the imbalance between congestion at exit gates, among those exits that are visible to the pedestrian. Furthermore, a social influence factor attends to neighbor behavior, which is a significant factor that influences exit-choice. An inertia parameter modulates the probabilistic trade-off over the factors influencing exit-choice changing to model the pedestrians' tendency to maintain initial choices. Finally, a CellEVAC leader influence factor attends to changes in the leaders' recommendations. For the final exit-choice decisions, we assumed that they are motivated by the distance to exit gates, congestion at exits, the flow of pedestrians to an exit, and the leaders' recommendations.

In the following, the eligibility mechanism, exit-choice changing, and exit-choice models are formalized.

3.1.1. Eligibility mechanism

Haghani and Sarvi (2019b) report that a pivotal element when modeling the decision changes is to give this chance to pedestrians for whom a change is physically possible. This mainly excludes the pedestrians confined by the surrounding crowd jam. Also, it is not very likely to make any change for a pedestrian who is progressing satisfactorily towards an exit gate. Therefore, as in Haghani and Sarvi (2019b), the following criteria were defined to determine whether or not a follower is eligible to make a changing decision. The local crowd density experienced by a pedestrian at a radius $r = 2m$ is measured. In order to be eligible, the following two conditions concerning local density and speed have to be met simultaneously. The simultaneous constraint of a minimum on the density and a speed maximum makes sure that the evacuee is experiencing a delay. Whereas the imposition of an upper bound on the density guarantees that the subject is not trapped.

$$1\,\text{peds}/\text{m}^2 < Local\,Density < 5\,\text{peds}/\text{m}^2 \text{ AND } Speed < 1\ \text{m/s}$$

The maximum $Local\,Density$ threshold is different to that used in Haghani and Sarvi (2019b), being increased from $3\,\text{peds}/\text{m}^2$ to $5\,\text{peds}/\text{m}^2$. We found by observing the behavior patterns in simulations that with low maximum thresholds, the influence of CellEVAC leaders' indications were not conveniently captured.

3.1.2. Decision changing model

The decision changing model is formulated as a binary logit with five parameters. The two alternatives considered are 'change' and 'not change' (of the exit choice). The utility of the 'change' alternative, U_{change}, is defined as Eq. (5), where V_{change} and ε_{change} are the systematic and error components.

The systematic component contains four variables and an alternative-specific constant. The first variable is the 'Congestion Ratio' (CongRatio), which measures the pedestrian density at each exit, $CONG_n$, relative to the density at the least congested exit, $CONG_{min}$, normalized by the $CONG_n$ value. The value of CongRatio tends towards 1 when the imbalance grows, so the probability of change increases.

'Visibility' (VIS) is defined as a binary categorical 0–1 variable that equals 1 if a less congested exit is visible and below a distance threshold from the position of the evacuee and is 0 otherwise. Intuitively, pedestrians are to change their decisions when alternative exits are known.

The third variable 'Social Influence' (SocInf) reflects that evacuees are to change decisions after observing others making a similar decision change. For a pedestrian who has chosen exit n initially, the binary variable SocInf takes the value of 1 if another evacuee has changed its exit decision from exit n within the last t seconds.

'IndicationChange' is the fourth variable, which models the influence that variations in leaders' exit indications can have when initiating a decision change process. When a pedestrian detects a change in the indication of the exit gate, the variable 'IndicationChange' will take the value 1, reinforcing the probability of exit change. In general, for a pedestrian to detect the recommendations of a leader agent, they must be at a distance less than a predetermined threshold d_{leader}. Of those leader agents within the distance threshold, for simplicity, in our work, the closest agent is taken as the influencing agent. 'IndicationChange' takes the value 0 when there are no influencing leader agents or there are no changes in indications.

Table 2
Configuration of the parameters of the decision changing model.

$Inertia$	β_{CR}	β_V	β_S	β_I
−7.5	3.5	0.8 (dist. threshold: 70%)	0.8 (time-horizon: 2 s)	1.75 (dist.threshold: d_{leader}=0–2 m)

Existing studies have confirmed that during evacuation simulations is crucial to maintain the decision change ratio at a low value, preventing simulated evacuees from 'flip-flopping' and producing unrealistic behaviors. This effect is captured with a negative value for the 'Inertia' constant.

$$U^p_{change} = V^p_{change} + \varepsilon_{change} = Inertia + \beta_{CR} \times \frac{CONG_n - CONG_{min}}{CONG_n} + \beta_V \times VIS + \beta_S \times SocInf + \beta_I \times IndicationChange + \varepsilon_{change} \quad (5)$$

Hence, the probability of the 'change' is obtained using the binary logit formula in Eq. (6).

$$P_{change} = \frac{1}{1 + e^{-V_{change}}} \quad (6)$$

The simplicity of this formulation keeps computational efficiency to an acceptable level when simulating large crowds, making potential calibrations possible. Moreover, if one desires to obtain the coefficient values using a simulation–optimization or try and error methodology, it is critical not to work with too many freedom degrees. Also, as suggested in Haghani and Sarvi (2019b), unit-less attributes help keep the model's generalizability level. For instance, $IndicationChange$ is based on the indications of the closest leader agent. Alternatively, we could have used a majority voting alternative to obtain the perceived exit gate indication.

The exit-choice changing model performance is impacted by the frequency at which the pedestrians revise their decisions. The simulation software uses an update cycle of 1 s to update the formulas. However, the $Inertia$ attribute modulates the changing ratio and when evacuees make new decisions. Even when a pedestrian is eligible, a decision change is not guaranteed. If the decision is to change, the initially chosen exit is excluded.

The base values of the model for the first four parameters are the same as that in Haghani and Sarvi (2019b), which produces good patterns of decision changing in a simulation environment. Alternative empirically calibrated values for these parameters can be used (Haghani et al., 2020), which produce similar results. The new β_I parameter was chosen based on an extensive experimental search process and set to 1.75, between β_{CR} and β_{V-S}, obtaining reasonable behavior patterns of decision changing (Table 2). The distance threshold d_{leader} was varied in the simulations between 0 m and 2 m, allowing us to modulate their degree of influence, which indirectly will depend on the number of leader agents in the evacuation scenario. It is important to note that it would have been possible to modulate the influence of the leader agents in the change of decisions by varying β_I *y* d_{leader} at the same time. However, we preferred balancing and minimizing the degrees of freedom in modeling the degree of the leader agents' global influence, by using d_{leader} only in the decision changing model, and another parameter in the exit-choice decision model.

3.1.3. Exit-choice decision model

The exit-choice model is formulated as a Multinomial Logit Model based with four attributes and as many alternatives as exit gates (Eq. (7)):

$$U_{pj} = V_{pj} + \varepsilon_{pj} = \beta_D \times DIST_{pj} + \beta_F \times FLTOEX_{pj} + \beta_C \times CONG_j + \beta_L \times LEADER_{pj} + \varepsilon_{pj} \quad (7)$$

$DIST_{pj}$ is the distance from pedestrian p to exit gate j, normalized in the range of 0–1 using the maximum distance measured to the different exits. $FLTOEX_{pj}$, estimates the pedestrian flow from pedestrian p to exit gate j, converted into a unitless attribute and confined within a fixed interval 0–1, dividing it by the maximum flow measured to the different exits. Therefore, parameter β_F is positive if pedestrians tend to follow other pedestrians.

The third attribute $CONG_j$ accommodates the congestion at exit gates, measured as a pedestrian density value, and normalized by the maximum density value found at the different exits. A negative value for parameter β_C would indicate that pedestrians avoid congested exit gates.

Finally, the $LEADER_{pj}$ attribute captures the followers' attitude towards the leader agents. This attribute is defined as a binary categorical 0–1 variable such that $LEADER_{pj}$ equals 1 if pedestrian p perceives an indication from a leader agent to choose exit j (e.g., pedestrians see the color corresponding to exit j in the led wristband of a leader agent in the vicinity), and is 0 otherwise. If there are not leader agents within the radius d_{leader}, $LEADER_{pj}$ takes value 0 for all j, so that utility will not depend on the indications provided by the CellEVAC system.

We may establish a distinction between environmental factors (distance, pedestrian flows, and congestion), and an exogenous factor (attitude towards leader agents using the CellEVAC system). Being our objective to evaluate the evacuation processes based

Table 3
Exit-choice model estimation results (statistical significance of 99%).

	Estimate	se	*t*-statistic
β_D (DIST)	−5.2002	0.2747	−18.93
β_C (CONG)	−4.5501	0.2414	−18.85
β_F (FLTOEX)	−0.0605	0.0108	−5.61
Log-likelihood (init)	−2083.6		
Log-likelihood (final)	−1831.838		
Pseudo ρ^2	0.1208305		
AIC	3669.68		
AICc	3669.82		
BIC	3685.62		

on the attitude of the pedestrians towards the leader agents, we decided to configure the exit-choice model by calibrating the environmental parameters β_D, β_F *y* β_C with real evacuation data, leaving as a configurable parameter β_L that allows modulating the influence of the indications of the leading agents in the choice of exit.

In order to calibrate the environmental parameters, we used the hypothetical-choice experiments carried out in Haghani et al. (2016), which replicates emergency evacuations with real participants. This data includes 2338 exit choice samples, in which the attributes of distance, congestion, pedestrian flow to visible exit, pedestrian flow to non-visible exit and exit visibility are considered. These data are used in Haghani et al. (2016) to obtain the parameter estimates of two exit-choice models: fixed-parameter multinomial logit, and random-parameter multinomial logit (mixed-logit). Because there are no obstacles in our evacuation scenario, and the exit-choice model does not include visibility parameters, we eliminated the samples that included non-visible exits in the choice set. In this way, the number of observations was reduced to 1503 and 167 decision-makers, including only attributes of distance, pedestrian flow to exits, and congestion. Data were normalized in the range 0–1 to accommodate the parameter estimation to our model requirements.

Our fixed-parameter multinomial logit model estimates were inferred from a simulated maximum log-likelihood procedure, using the 'mixl' open-source R package for estimating complex choice models on large datasets (Molloy et al., 2021). As expected, all the estimated coefficients took negative values, with a more relevant influence of the distance and congestion attributes (Table 3).

In all the experimental setups, we found it reasonable that pedestrians following the indications of leaders were committed during the entire evacuation process, while leaders followed the indications of the CellEVAC system.

3.1.4. Followers' choice of speed

During evacuation simulation, leader and follower agents' motion is governed by the Social Force Model, where the chosen exit gate determines the directional component. For leader agents, exit choices are determined by the indications provided by the CellEVAC system, while the eligibility mechanism, exit-choice changing, and exit-choice decision-making processes determine follower agents' exit choice. In this research, we assume that leaders are instructed to walk during the evacuation at a recommended average speed to guide other pedestrians.

It is well known that the individual choice of speed (Fridolf et al., 2013) is one of the main factors that affect the evacuation processes and that environmental and attitudinal factors condition it. In our research, and for follower agents, a speed choice mechanism has been designed that depends on the pedestrians' attitude towards the leader agents' indications. Being our main objective to model and study the influence of leaders on pedestrians, it made sense to adapt and model both the choice of exit and speed. In this way, the follower agents have a predetermined preferred speed, which will be the agent's speed in free-flow conditions. Indeed, the actual speed during the simulation will depend on the congestion conditions, although the agent will always try to advance at the predetermined preferred speed. However, when a follower has a leader in the vicinity, and the leader's indication coincides with the agent's choice, we assume that the follower adapts to the leader with a reasonable probability, and so, his/her speed is also adapted to the current leader's speed. Whenever the followers are not under the influence of any leader agent or make an exit choice that differs from the recommended exit gate, the preferred speed switches to the predetermined speed.

Note that we make no ambiguous categorical assumptions about the underlying motivation that determines the preferred speed of the follower agents. Our goal is to model a possible situation of urgency in which they tend to walk fast. We, therefore, explicitly avoid using terms like "panic" to justify the followers' desired speed, as recommended in Haghani et al. (2019).

4. Evacuation efficiency: evacuation time, measurement of congestion and risk

The metrics most often used in measuring the efficiency of evacuation processes have been the total evacuation time and the average individual evacuation time. From the perspective of crowd evacuation management, many of the evacuation control systems described in the literature aim to optimize these values (Abdelghany et al., 2014; Zhong et al., 2016b). However, when considering this performance measure exclusively, the risk inherent to the speed induced in pedestrians is neglected. If we consider, for example, a control mechanism design based on a simulation–optimization process, and the risk or danger is not modeled, the mechanism configured to optimize the evacuation time in the simulation environment may distort the evacuation process in a real environment where dangerous situations may appear. Furthermore, other more subtle aspects may emerge, such as the number of decision

changes. A mechanism that causes an excessive number of decision changes could optimize the evacuation time in the simulation environment but not be applicable in a real environment due to the stress produced.

In this work, we have considered these aspects, and on the one hand, the CellEVAC system is optimized by combining evacuation time and accumulated density variance at the exit gates (Eq. (3)). It is well known that the dynamics of flow are governed by physical interactions generating hazardous situations when density becomes too large. Evacuation systems should maintain density under a critical value to reduce this effect. Thus, by minimizing the variance, we balance the outflows and the accumulated density at the exits. Moreover, the number of decision changes generated by CellEVAC is modulated by the Inertia parameter $\beta_{In}(t)$, keeping the ratio of changes under an acceptable threshold. On the other hand, to evaluate the efficiency of evacuation processes, we incorporate evacuation time factors and congestion measures for risk assessment. In the following, we present in detail the methodology used to measure the efficiency of the simulated evacuation scenarios in terms of congestion level and risk.

4.1. Measurement of congestion and risk

Density has been typically used to evaluate crowd motion and composition and judge critically intrinsic risk in pedestrian crowds, though this is not the only relevant property (Helbing and Mukerji, 2012; Dambalmath et al., 2016). As stated in Feliciani and Nishinari (2018), the limiting capability of density to explain the dynamics of crowds lies in its static nature. Crowds become particularly dangerous when shock waves propagate, thus creating an alternation of large forces from multiple directions (Helbing et al., 2007; Helbing and Mukerji, 2012).

In Geroliminis and Daganzo (2008), Geroliminis and Sun (2011), the authors study the existence and properties of macroscopic fundamental diagrams at urban scale for vehicle networks, connecting flow and density. Saberi and Mahmassani in Saberi and Mahmassani (2014) introduced the notion of area-wide Fundamental Diagrams for pedestrian crowds, which formulates the relation between pedestrian density and the average flow (number of pedestrians per meter and per second) in an area. Area-wide FD was later renamed pedestrian Macroscopic Fundamental Diagram (pMFD) in Hoogendoorn et al. (2018), which studies the influence of spatial density variation on pedestrian flow.

Therefore, although the pedestrian MFD has proven to be a powerful concept in understanding and controlling pedestrian flow dynamics, the interpretation of the fundamental diagrams as a congestion classification tool should be treated cautiously. In Feliciani and Nishinari (2016, 2018), it is highlighted that similar fundamental diagrams do not allow, for example, to distinguish different types of bidirectional flows. In any case, this problem may be less critical in scenarios where the goal is to compare and analyze the risks of flows with similar patterns of directionality.

Fruin proposed one of the first approaches to classify congestion (Fruin, 1987), the Level of Service (LOS), with which different types of facilities are rated based on qualitative observations. Each LOS is provided with numerical values for density and flow expected, changing from facility to facility. The main disadvantage of the LOS is that it is not universal, and implementations for real-time crowd control are complicated.

For the particular purpose of risk measurement at exit gates, we proposed in Lopez-Carmona and Paricio Garcia (2021) a safety metric based on the derivation of local fundamental diagrams. For constructing these diagrams, pedestrian flows were induced with a significant variation in spatial density, including queue build-up, recovery, and blocking phases. We aimed to generate shockwaves and a representative number of points in the fundamental diagrams. Following this procedure, we obtained FDs, which were parameterized using density thresholds attending to the different phases observed. Using these thresholds, we derived a formula to estimate a “safety” metric to evaluate the risk or danger during the evacuation at the different exits.

Focused on a macroscopic view, Feliciani and Nishinari (2018) propose a new method to measure pedestrian congestion and the intrinsic risk in pedestrian crowds. The different congestion levels are estimated based on the rotational of the velocity vector field obtained from the collected trajectories of pedestrians. This congestion level is defined as:

$$Cl = \frac{\max(r_z) - \min(r_z)}{|\vec{v}|}$$

where $\max(r_z)$ and $\min(r_z)$ are the maximum and the minimum of the rotational over a region and $|\vec{v}|$ is the average absolute velocity in that region. The congestion level defined as a function of a velocity vector field allows determining the organizational degree and the dynamical nature of pedestrian crowds. In order to estimate the risk of the crowd, the crowd danger is defined as:

$$Cd = Cl \cdot \rho$$

where ρ is the local density. Authors do not define critical values for crowd danger above which accidents are likely to happen, but a practical scale for actions to be taken at different levels of crowd danger can be defined. Feliciani et al. show that “crowd danger” provides a more universal and consistent description of crowd motion. However, in evaluating evacuation processes, the need to use more or less sophisticated evaluation metrics will depend on the aim of the evaluation. If the objective, as is our case, is to compare evacuation processes with similar directionality patterns, more straightforward density-based metrics based on MFD for broad regions and cumulative density measurements at exits (Feliciani et al., 2020) may be sufficient to compare crowd risk and performance.

To estimate the intrinsic risk of the pedestrian crowd from a macroscopic perspective, in our work, we have used the “crowd pressure” metric formulated by Helbing et al. (2007), defined as the local variance of velocity multiplied by the corresponding density given by:

$$Cp = \rho \cdot Var(v)$$

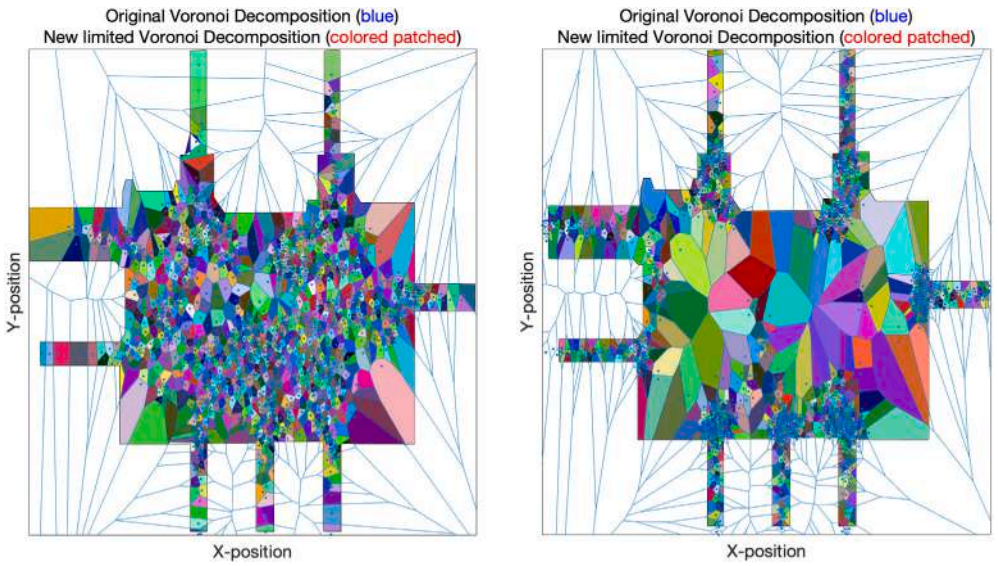

Fig. 1. Example of Voronoi diagrams for Madrid Arena.

where ρ is the local density and $\mathrm{Var}(v)$ is the local temporal variation in pedestrian speed. Using this quantity Helbing et al. identify regions responsible for "crowd turbulence" (Helbing et al., 2007; Helbing and Mukerji, 2012). To determine the local density we use the concept of Voronoi diagrams (Steffen and Seyfried, 2010; Zhang and Seyfried, 2013) to the microscopic data from simulations. Fig. 1 shows an example of two Voronoi diagrams for our evacuation scenario. In a Voronoi diagram each region represents a single pedestrian and includes all locations closer to the pedestrian than to any other pedestrian. Each point in the diagram shows the location of a pedestrian i at time instant t_k. Being Ω_i the area available to the pedestrian, we modify the standard Voronoi diagram in such a way that $A = \cup_{i=1}^{n} \Omega_i$, where A is the walking area (Hoogendoorn et al., 2018). In Fig. 1, we may see that though the diagrams extend to infinite, the cells are restricted to the evacuation area. Once computed the Voronoi diagram, the pedestrian specific density is defined as:

$$\rho_i(t_k) = \frac{1}{|\Omega_i(t_k)|}.$$

The average density of pedestrians at time t_k is computed by averaging the pedestrian specific densities:

$$\rho(t_k) = \frac{1}{n} \sum\nolimits_{[i=1]}^{n} \rho_i(t_k),$$

where n is the population of agents in the evacuation area. If our aim is to calculate the flow vs. density MFD, the region-wide instantaneous mean speed is determined by averaging the speed of all pedestrians at time t_k. On the other hand, to estimate the crowd-pressure vs. density MFD, the region-wide instantaneous mean speed variance is obtained by averaging the variance of speed of all pedestrians.

We used the crowd-pressure vs. density MFDs and a predefined crowd-pressure threshold to compare the risk of different evacuation processes from a wide region perspective. Intuitively, an evacuation scenario will be more or less dangerous, dependent on the number of crowd-pressure points above the threshold.

In addition to the macroscopic evaluation, the evaluation of scenarios collected in this work includes evaluating the local risk at the exit gates. Here, we have opted for a simple metric based on a measure of the cumulative density at each exit gate (Murakami et al., 2020).

5. Microscopic simulation analyses

Here, the experimental results using microscopic simulation are shown and discussed. In all the simulations, the evacuee population consisted of 3400 pedestrians on the ground floor, the facility's maximum capacity. Followers were configured to move at a speed in the range 1.24–1.86 m/s under free-flow conditions, and the leaders were instructed to move at a lower average speed of 0.62 m/s. We aimed to model a very acute emergency condition in which evacuees tend to move at high speed in the presence of leader agents coordinating the evacuation at a lower speed.

Due to the stochastic nature of the evacuation simulation processes, we ran 10 simulations to obtain each Macroscopic Fundamental Diagram, with a sampling period of 2.5 s to extract each flow vs. density or crowd-pressure vs. density point. To estimate the evacuation time, the average evacuation time, average number of decision changes, safety (risk), and cumulative

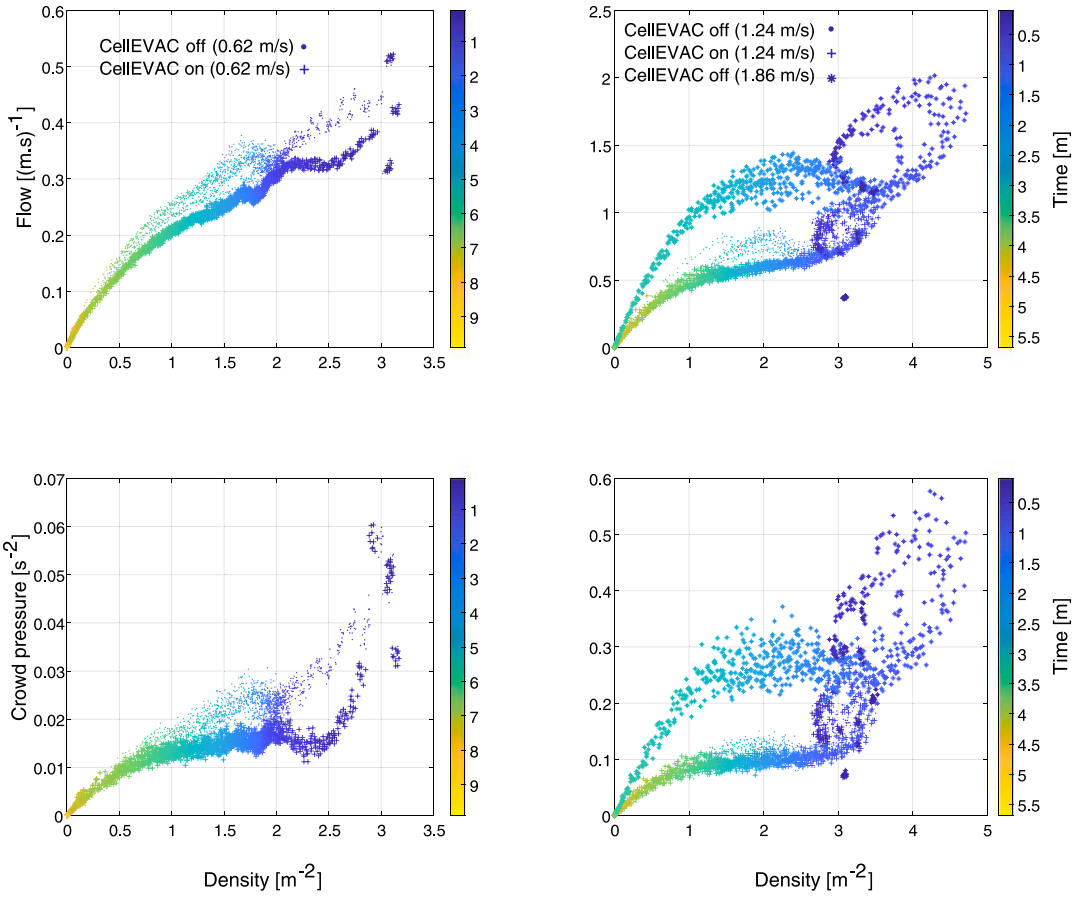

Fig. 2. Flow vs. density (first row) and crowd-pressure vs. density (second row) MFDs. Each plot shows the macroscopic fundamental diagrams for different pedestrian preferred speeds, in evacuation scenarios in which all the pedestrians are leaders and use the CellEVAC system (CellEVAC on), or all the pedestrians behave according to the calibrated followers' behavior model (CellEVAC off). The color of each point and the color bar provide a temporal view of the evacuation process. The sampling period is 2.5 s. (For interpretation of the references to color in this figure legend, the reader is referred to the web version of this article.)

density at exits, we used the replication algorithm described in Section 2.3, with a minimum of 20 and a maximum of 50 simulations (replicas).

We first investigated how evacuation performance could be influenced by the CellEVAC system and the pedestrians' speed. In these simulation experiments, all-nothing configurations were tested, in which there were only leaders (CellEVAC on) or followers (CellEVAC off), with a predetermined target speed. The pMFDs with timestamps in Fig. 2 show that for low speeds (0.62 m/s), the use of CellEVAC results in similar evacuation times but a significant improvement in crowd pressure. The pressure differences become less significant for speeds around 1.24 m/s, with a slight improvement appearing in the range of densities 1–3 m^{-2}, which appear in the evacuation scenario in the time interval from 1.5 to 3.5 m. The simulation of a scenario without CellEVAC and a speed of 1.86 m/s confirms a significantly lower evacuation time but a pressure that triples the values achieved in the previous experiments. In all cases, a hysteresis phenomenon is observed with very high-pressure values, which indicates a significant risk zone at the beginning of the evacuation process. These experiments confirmed the viability of using CellEVAC to control the evacuation time and safety from a broad region perspective.

Next, we evaluated the performance of CellEVAC as a leader-based guidance system for different leader ratios and follower behaviors. Thus, we modeled five types of evacuation scenarios determined by the followers' preferred speed, the β_L parameter of the exit-choice module that modulates the influence of leaders on exit-choice, and the distance at which a follower can detect a leader.

Two evacuation scenarios assume homogeneous follower behavior with a preferred speed of 1.86 m/s. The first scenario, Low leader-following level (Low LF), assigns $\beta_L = 0$ and $d_{leader} = 1$ m, which means that followers adapt to leaders' speed when they are very close to a leader and have chosen the same exit gate. In the second homogeneous scenario, called High leader-following (High LF), followers are trained to follow the indications of the leader agents (High LF), parameters $\beta_L = 10$ and $d_{leader} = 2$ m, which means that followers tend to imitate the leader behavior.

The other three evacuation scenarios study heterogeneous populations of followers. In these scenarios, individual followers' preferred speeds are drawn from a uniform distribution $U(1.24-1.86)$ at the beginning of the evacuation process. Also, the distance at

Table 4
Evacuation scenarios for different follower behaviors: Low LF—homogeneous Low leader-following; High LF—homogeneous High Leader-Following ; Type A—fully heterogeneous; Type B—heterogeneous LF trend; Type C—heterogeneous HF trend.

	Preferred speed (m/s)	d_{leader} (m)	β_L
Low LF	1.86	1	0
High LF	1.86	2	10
Type A	$U(1.24-1.86)$	$U(1-2)$	$U(0-12)$
Type B	$U(1.24-1.86)$	$U(1-2)$	$Beta\ (\alpha=1,\beta=10)$
Type C	$U(1.24-1.86)$	$U(1-2)$	$Beta\ (\alpha=10,\beta=1)$

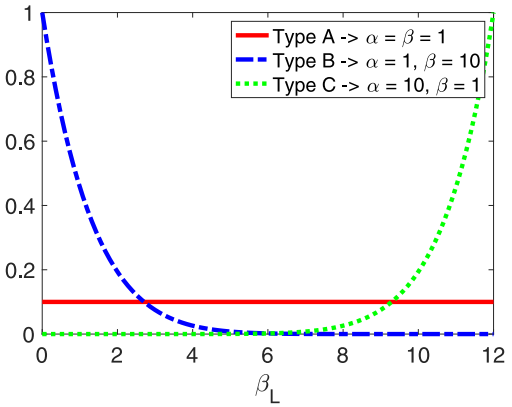

Fig. 3. Probability density functions for the β_L parameter in the scenarios Type A-B-C.

which each follower can detect leaders varies dynamically during the evacuation according to a uniform distribution $d_{leader} = U(1-2)$. The three scenarios are distinguished depending on how the β_L parameter values are distributed across the population of followers. In the Type A scenario, β_L is drawn from a uniform distribution $U(0-12)$ to describe a fully heterogeneous population of followers. The Type B scenario uses a left-skewed Beta random distribution with parameters $\alpha = 1, \beta = 10$ in the range 0–12, which defines a general trend to non-cooperative behavior. Finally, the Type C scenario defines a cooperative behavior scenario with a right-skewed Beta random distribution with parameters $\alpha = 10, \beta = 1$ in the range 0–12.

Table 4 and Fig. 3 summarize the configurations of the evacuation scenarios.

Fig. 4 reports the pMFDs obtained for several homogeneous scenarios. We observed a clear benefit in evacuation safety (low crowd pressure) when followers were trained and for evacuation scenarios with many leader agents. However, lower levels of crowd pressure come at the cost of higher total evacuation time, which may double its value for a leader ratio of 10% (340 pedestrians). However, note that the leaders' velocity were configured to a very low value, exaggerating these values. Interestingly, there exist an evacuation time and average evacuation time peak between the minimum and maximum leader ratio (50% in Low LF and 20% in High LF scenarios).

Fig. 5 shows the results obtained for each evacuation scenario. Evacuation time and average evacuation time follow the same trend in all the scenarios, with distributions of values that depend on the homogeneity of the populations. In the Low LF scenario, the peak is around 50% of the CellEVAC/leader ratio, while the peak moves around the 20% ratio in the High LF scenario. This is consistent with global coordination with leaders is easier in the High LF scenario. Interestingly, as the number of leaders increases from these CellEVAC ratios, evacuation time and average evacuation time decreases. These results suggest that more effective and controlled coordination benefits the evacuation time. In the heterogeneous scenarios, the measurements of evacuation time and average evacuation time are relatively similar, slightly lower than for the High LF scenario.

Overall, experiment results showed a significant influence of leader ratios on the number of exit-choice changes, with a linear increase for higher ratios. This comes from the fact that with many leaders, followers' probability of contacting different leaders during evacuation increases. We also observed that the number of exit-choice changes for trained followers was less for the same leader ratio, which appears to be because a change of leader is less likely.

To measure the risk of an evacuation simulation, we used an arbitrary crowd-pressure threshold of $0.04\ s^{-2}$ and calculated the ratio of points in the MFD below the threshold (safety value). This threshold was reported in Helbing et al. (2007) to denote crowd pressure from which fatalities occur. This gives us a rough and simple estimation of safety with values between 0 and 1. Thus, the safety value gives us the proportion of evacuation time in which there is no apparent risk situation. However, note that this is an estimate valid for comparison purposes, but that in no case does it allow a precise determination of the actual probability of accidents occurring. Remarkably, the experimental results showed a significant increase in safety for higher leader ratios and a High LF level. In the heterogeneous scenarios, we also observed a clear benefit in safety for leader rates above 10%. It confirmed our hypothesis about the usefulness of having leader agents using CellEVAC and informed pedestrians to improve evacuation safety, even in heterogeneous scenarios with uneven distributions of trained pedestrians.

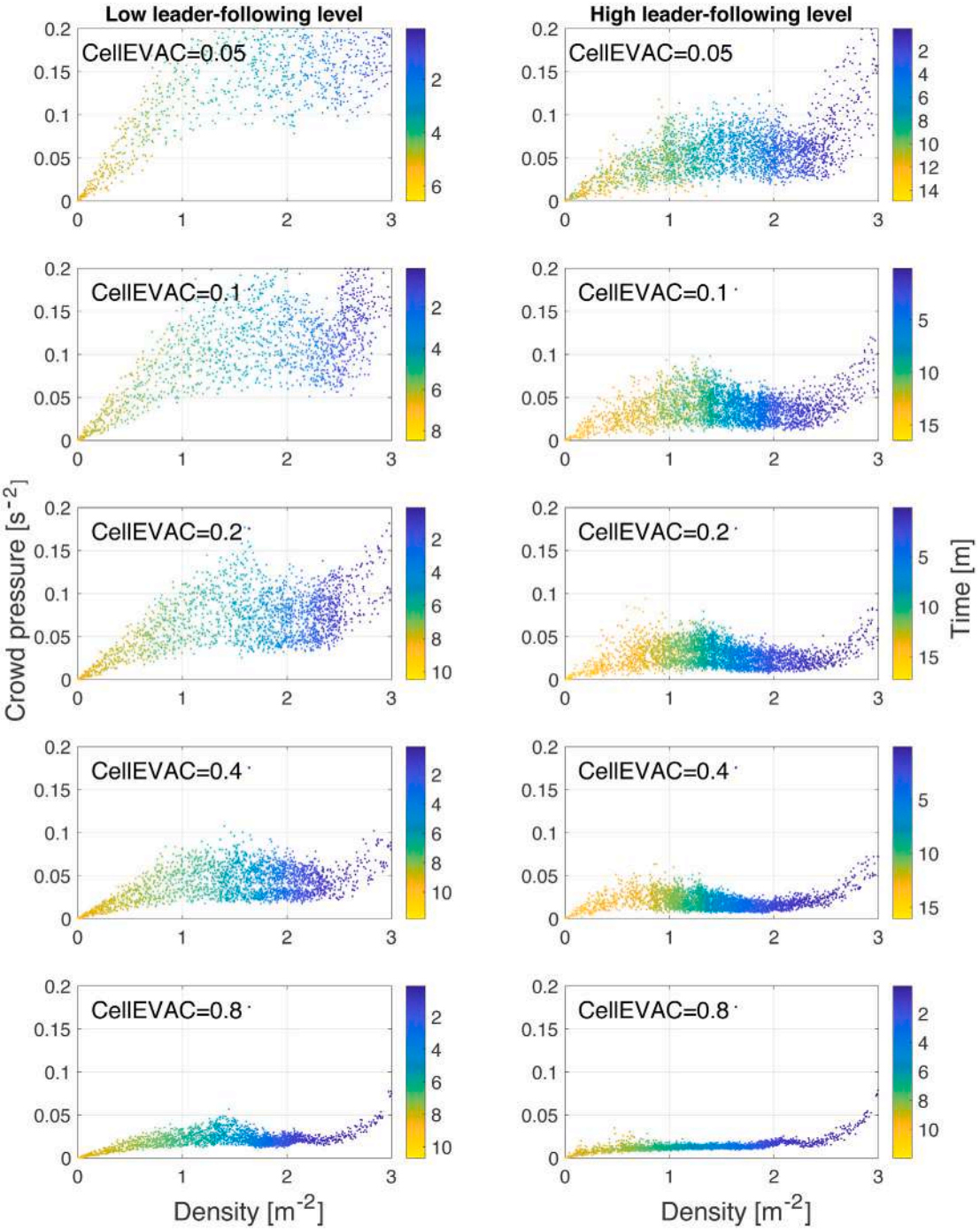

Fig. 4. Crowd-pressure vs. density MFDs for different leader ratios (e.g., $CellEVAC = 0.8$ defines a ratio of 80%) and leader-following levels. In all the evacuation scenarios, leaders' and followers' preferred speeds are set to 0.62 m/s and 1.86 m/s, respectively. In the MFDs on the first column, parameters $\beta_L = 0$ and $d_{leader} = 1$ m, defining a low leader-following level. In the second column, $\beta_L = 10$ and $d_{leader} = 2$ m, with followers exhibiting a high leader-following level.

As an example, the performance analysis results for each individualized exit gate have been summarized in Fig. 6, which corresponds to the Low and High LF scenarios. The box-plot shows the cumulative densities for leader ratios from 0 to 20%, revealing significantly worse performance when not using the CellEVAC system (red boxes). Also, the cumulative density at exits is lower when pedestrians exhibit a high LF level, confirming the positive effect on safety at exit gates of having informed pedestrians. However,

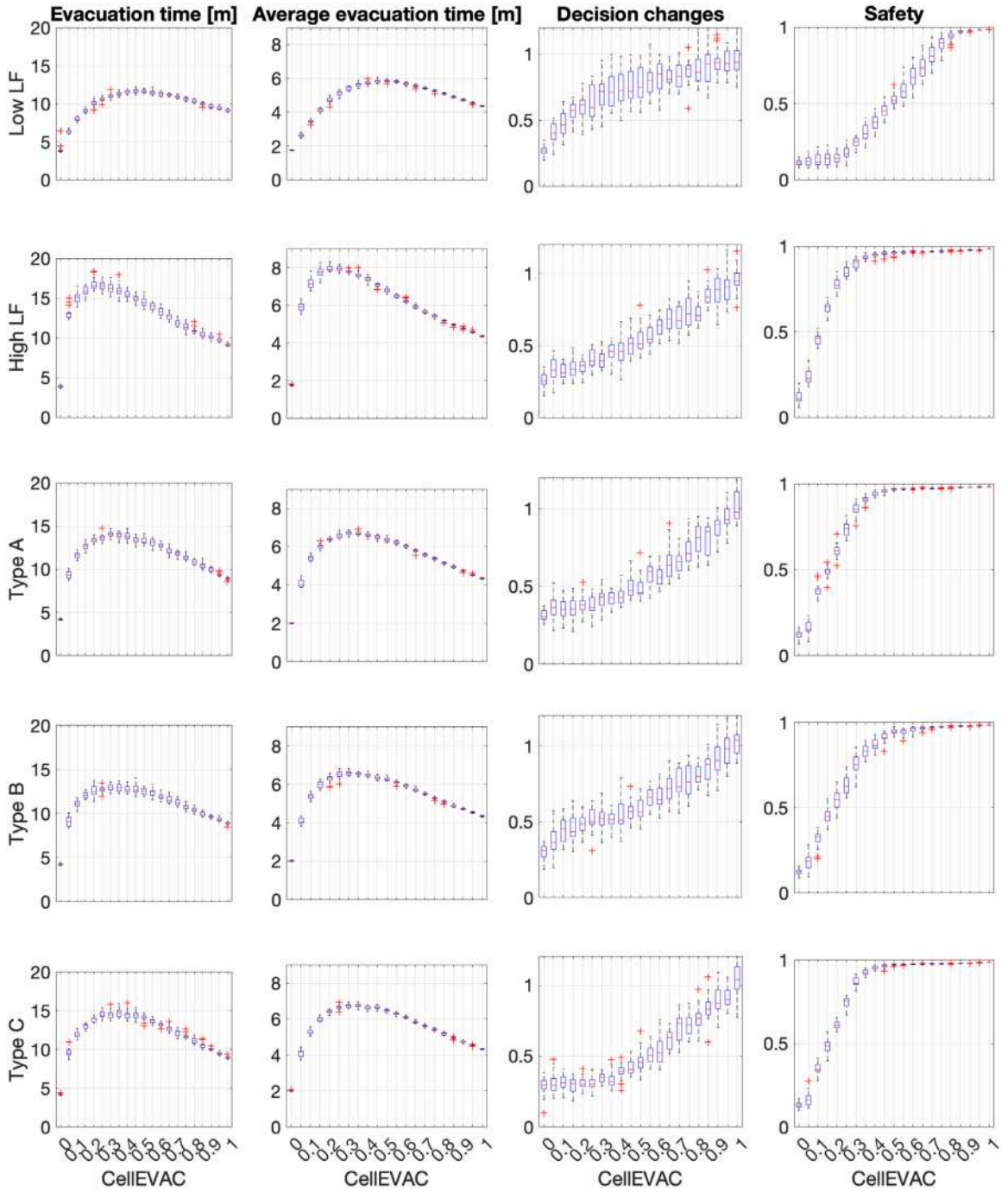

Fig. 5. Box-plots of evacuation time, average evacuation time, the average number of decision changes per pedestrian, and safety for different leader (CellEVAC) ratios and evacuation scenarios (Low LF, High LF, Type A, Type B, and Type C). The horizontal axes define the different leader ratios in the pedestrian population.

there is no evidence of differences in safety for informed agents when the number of leaders increases. In conclusion, the most crucial aspect regarding safety at exits is to have informed pedestrians to follow leader agents.

To evaluate the influence of leaders' velocity on evacuation performance, we developed the same experimental analysis varying the speed of the leader agents, going from 0.62 to 1.24 m/s. The results of these experiments confirmed similar trends and correlations in all cases. As expected, the main performance differences are given by shorter evacuation times, lower levels of overall safety, and higher accumulated density values at the exits.

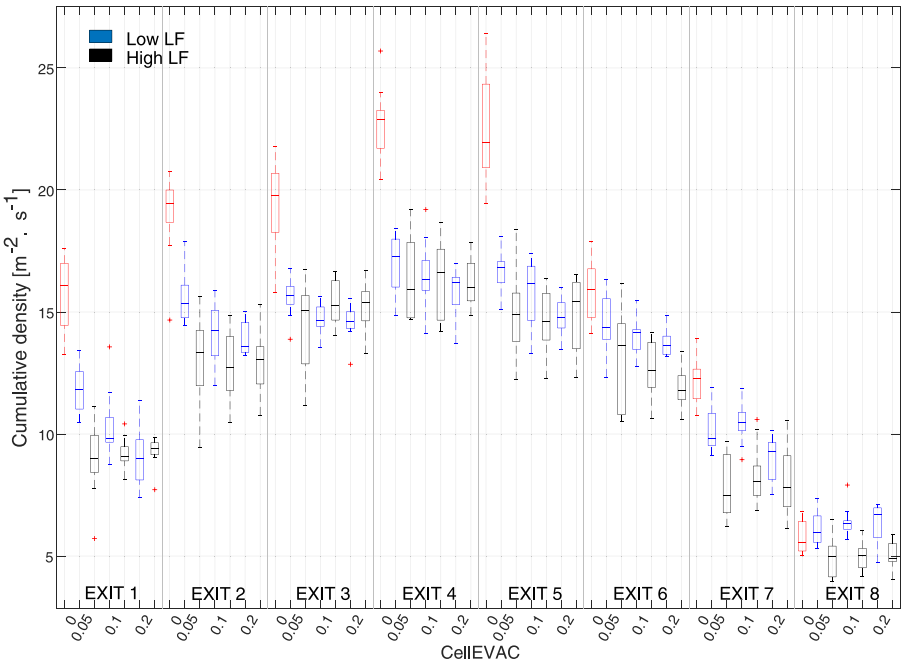

Fig. 6. Cumulative density at exit gates. In all the evacuation scenarios, leaders' and followers' preferred speeds are set to 0.62 m/s and 1.86 m/s, respectively. Red boxes represent the cumulative density for evacuation scenarios without leader agents. The horizontal axis groups the results in pairs for Low LF and High LF levels (blue–black boxes). Each pair of blue–black boxes shows the results for a given leader ratio (0.05, 0.1, 0.2). (For interpretation of the references to color in this figure legend, the reader is referred to the web version of this article.)

The outcomes of single-run simulations for different homogeneous evacuation scenarios are shown in Fig. 7. As expected, in a scenario without leaders and a target speed of 1.86 m/s, the evacuation time is short at the cost of high-density values at exits. In contrast, when all pedestrians use the CellEVAC system, evacuation time increases slightly with a significant decrease in the density values. For scenarios with a leader ratio of 20%, as expected, evacuation time increases, and density curves flatten. Behind the flattening of the curves of density is that followers' speed adaptation to the leaders' speed produces a grouping effect that benefits the arrival of pedestrians to the exit gates in a coordinated way.

Finally, for illustrative purpose, snapshots of the single run simulation experiments for the "NL (No Leader agents)", "CellEVAC", "20% Leaders LF", "20% Leaders HF" configurations are presented in Figs. 8 and 9. As expected, with "CellEVAC," a highly organized behavior pattern is observed, a lower spatial density variation, and lower density at the exit gates when compared to the "NL" scenario. In the CellEVAC guidance scenarios, there are significant differences between the scenario with LF follower agents and the scenario with HF agents. In the HF scenario, the evacuation process is more homogeneous, inducing less crowd pressure at the exits. It is observed how the tendency of the follower agents to adapt to the leading agents causes a grouping that coordinates the evacuation process in terms of exit choice and target speed. Overall, these results have strengthened our confidence in the CellEVAC system as an effective adaptive leader-based crowd guidance system.

6. Discussion

Our use of an adaptive guidance system based on cells and LED wristbands (CellEVAC) as a leader-based evacuation management system has proven its efficiency in terms of safety and number of decision changes at the cost of higher evacuation times. Interestingly, by varying the target speed of the leader agents we may balance the expected evacuation time against the intrinsic risk of the crowd. The proposed system has as main requirements that the leaders are trained to move at a predetermined target speed and attend the CellEVAC exit indications. Moreover, the follower agents are expected to know a priori the need to follow the instructions of the closest leaders. These requirements could reasonably be satisfied by hiring a trained evacuation staff and by advertising the leaders' follow-up recommendations on the event website, signage, and tickets. Up to our knowledge, this is the first leader-based evacuation guidance system based on LED wristbands for the adaptive recommendation of exit gates. We strongly believe that this proposal has high potential due to its simplicity, with a human–machine interface which provides simple instructions, and a deployment cost and complexity expected to be small.

The proposed behavioral model for follower pedestrians, structured in 3 layers as in Haghani and Sarvi (2019b), has allowed us to model the tendency of evacuees to follow the leader's guidance in a simple and straightforward manner. In our work, this modeling has been restricted to modulate the imitation of the leader's speed and choice of exit. Both the exit changing and exit choice models are parameterized with distance, congestion, and inertia value (only the exit changing module). Keeping the proposed

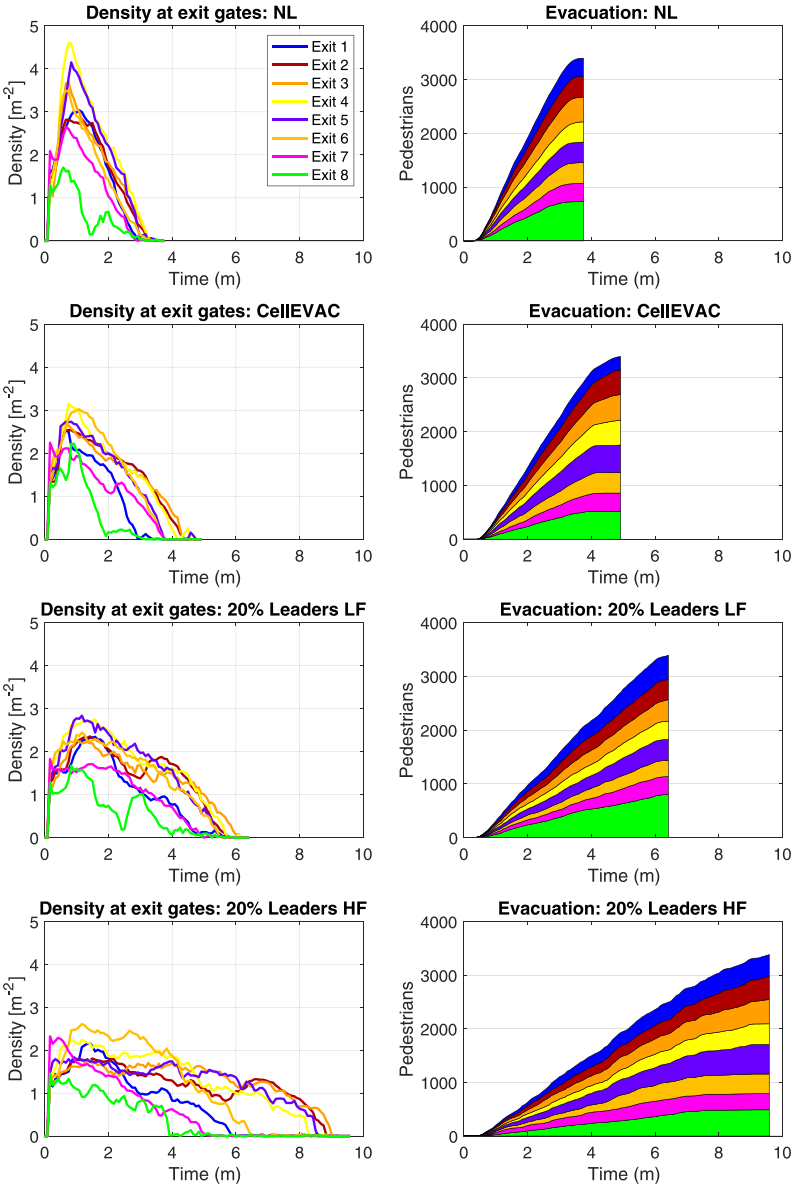

Fig. 7. Evolution of density and pedestrian outflow at exit gates for different scenarios: (1) NL: there are not leader agents, (2) CellEVAC: all the pedestrians are leader agents, (3) 20% Leaders LF: 20% of pedestrians are leaders, and followers exhibit a low following-leader level, (4) 20% Leaders HF: 20% of pedestrians are leaders, and followers exhibit a high following-leader level. In all the evacuation scenarios, leaders' and followers' preferred speeds are set to 1.24 m/s and 1.86 m/s, respectively.

structure, it would be possible to model different evacuation behaviors easily by partially modifying or extending the discrete choice models of the last two layers.

Another relevant aspect to discuss in terms of modeling the degree of imitation relates to the distance thresholds used to assess that a leader is visible and is considered in the exit change and exit choice decision processes. The strategy followed in our work has been to keep the model as simple as possible. The larger or smaller population of leading agents determines the population's overall tendency to follow CellEVAC instructions for a predefined distance. An exciting extension of the model of follower agent behavior on leader visibility would be given by a graduation of the level of visibility, determined from the density of pedestrians in the direct line of sight to the leader.

We believe that the experimental results, reasonably reflect the viability of CellEVAC as a guidance tool in an evacuation context with two different populations, leaders and followers. For practical purposes, one might wonder if it is more effective to have expert agents who give recommendations to nearby groups of evacuees without LED wristbands or have an entire population of evacuees without leaders, but with LED wristbands and little or no degree of training. This aspect is appealing and would require

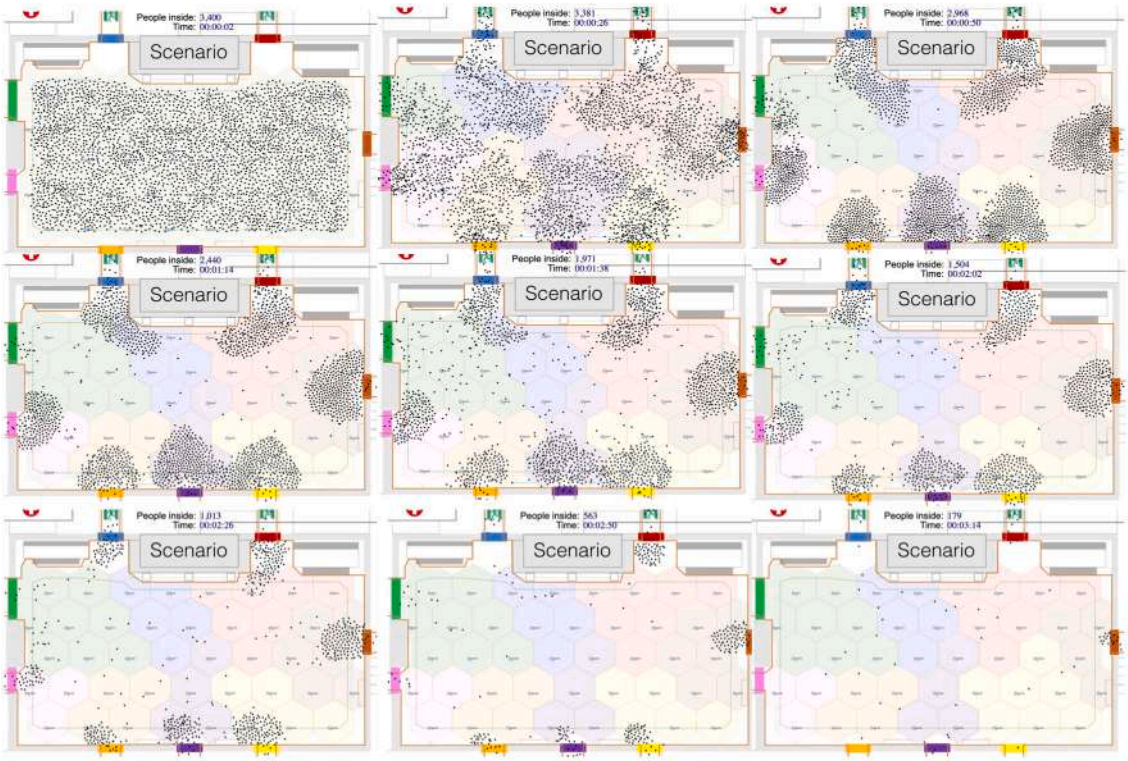

(a) NL (No Leader agents).

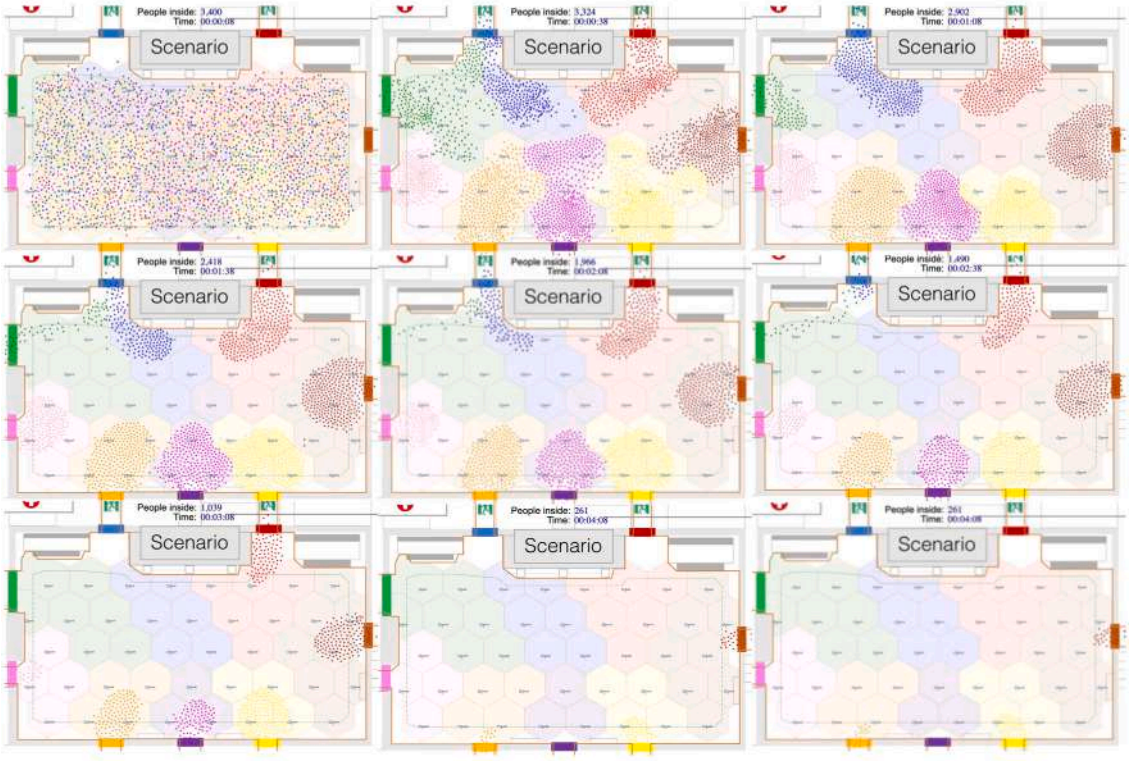

(b) CellEVAC 100%.

Fig. 8. Snapshots of two evacuation simulations: (a) where there are followers only, and their preferred speed is set to 1.86 m/s; (b) where there are leaders only, and their preferred speed is set to 1.24 m/s. Black dots represent follower agents.

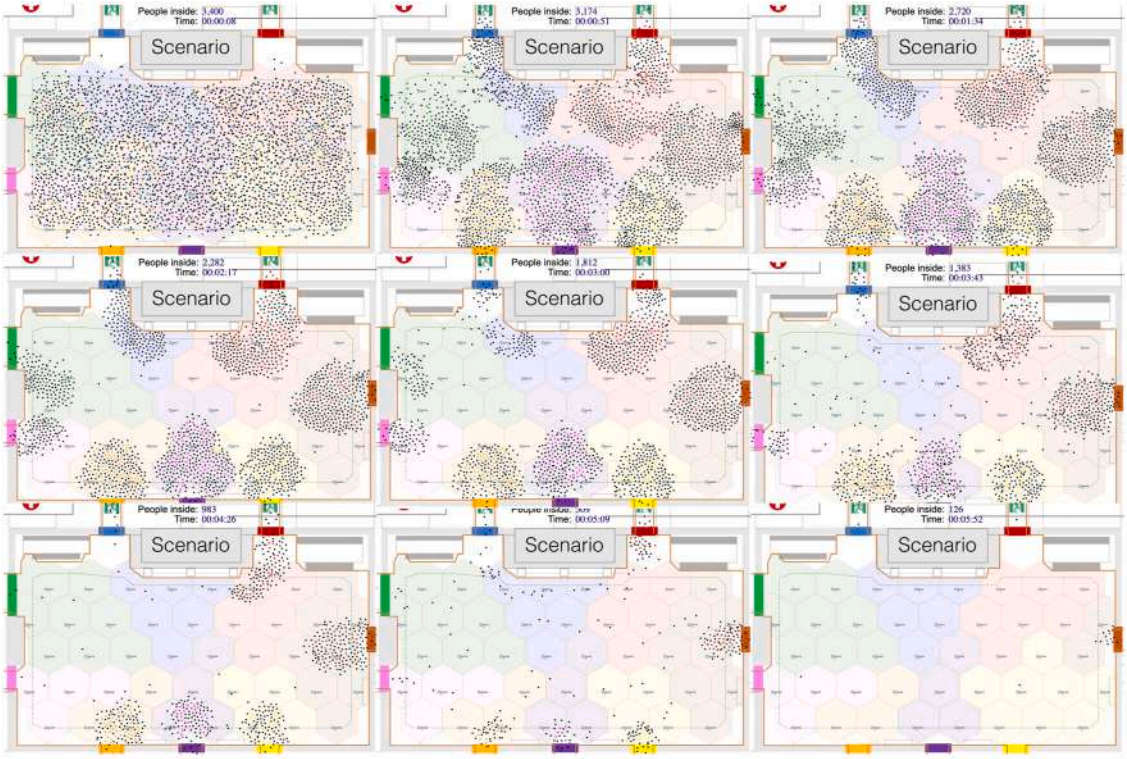

(a) Low leader-following level.

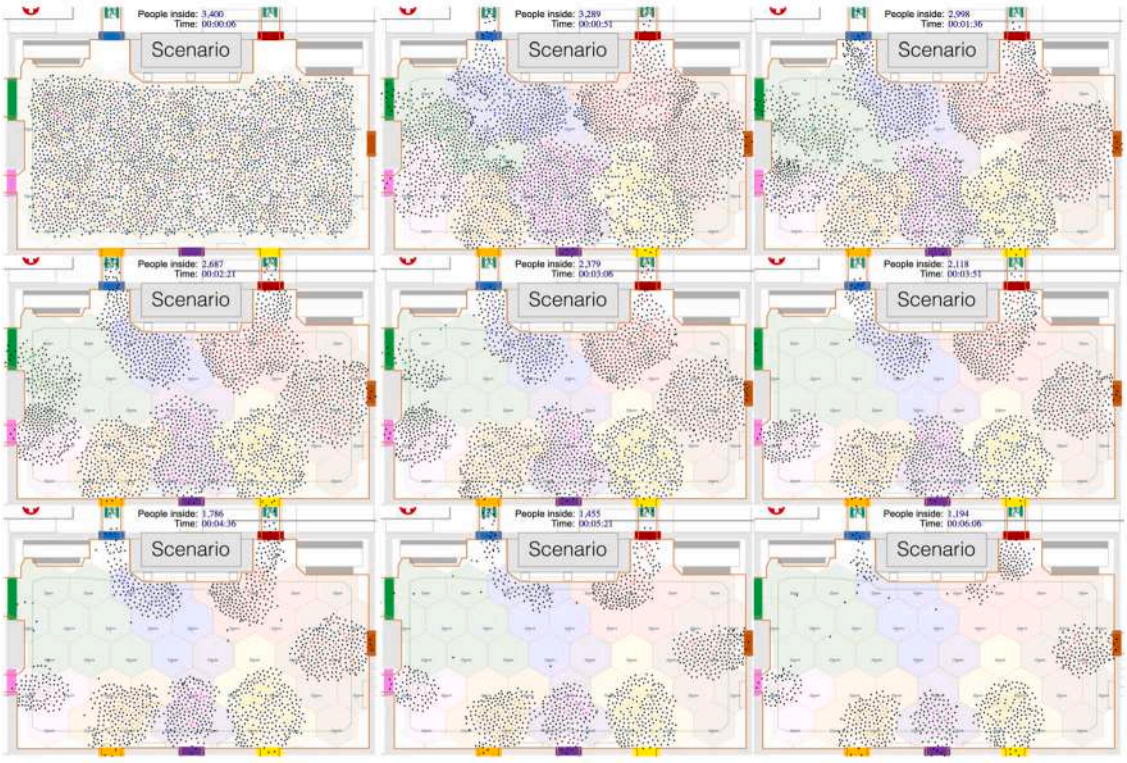

(b) High leader-following level.

Fig. 9. Snapshots of two evacuation simulations with a leader ratio of 20%. Leaders' and followers' preferred speeds are set to 1.24 m/s and 1.86 m/s, respectively.

laboratory simulations or hypothetical-choice experiments. Our intuition is that in emergencies characterized by high levels of stress, receiving human instructions is particularly important to promote coordinated evacuations and to improve safety (Lopez-Carmona and Paricio Garcia, 2021).

Regarding the simulation–optimization process to configure CellEVAC, we considered an evacuation scenario where all evacuees used the system, and there were no blockers or counterblows (e.g., emergency services). Thus, exciting aspects of studying are how the proportion of leading agents and the consideration of blockers or counterblows influence the optimal configuration of CellEVAC. In general, considering a scenario with a proportion of predetermined agents, behaviors, and expected environmental factors improves the system's operation. Also, note that our optimization goal implied minimizing the evacuation time and the balance of outflows. However, other aspects could replace these goals depending on the specific application.

Finally, another of our main objectives was to use a global safety measure as a performance metric. As suggested in Hoogendoorn et al. (2018b), pedestrian MFDs can be used in several applications such as the network-wide determination of Level-of-Service, the crowd control, or the modeling of the coarse dynamics in pedestrian networks. For the specific purpose of measuring congestion and risk in pedestrian crowds from a network-wide perspective, we have used pMFDs taking the crowd pressure as the reference value. However, we are aware that other alternatives can measure intrinsic risk, such as the crowd-danger metric based on the rotational velocity field proposed in Feliciani and Nishinari (2018). Also, we have used an arbitrary threshold to estimate safety, which is valid for comparison and analysis purposes when the different flow dynamics to compare are similar. However, if the goal is to estimate a precise probability of accidents happening, we would need a calibration technique to set adequate thresholds.

7. Conclusions

This paper has proposed a leader-based adaptive evacuation guidance system based on indoor positioning in cells and LED wristbands (CellEVAC) used by trained evacuation staff. The system provides optimal exit indications showing different colors in the wristbands, which allow leaders to choose a specific exit gate dynamically. The system requires trained leaders to move at a predefined average speed, thus guiding evacuees to the appropriate exit and minimizing the inherent risk of the crowd. Using color codes in LED wristbands, the interpretation of guidance indications is greatly simplified, essential in stressful environments found typically during evacuations (Lopez-Carmona and Paricio-Garcia, 2020).

The proposed system architecture divides the facility into cells such that evacuation staff (leaders) in a cell receive the same recommendations. An indoor positioning system provides evacuation staff location-aware capabilities through the wristbands. The system's core is the decision logic module that monitors the environment, decides on allocating exit gates (colors) to cells, and sends this allocation throughout a broadcast communication channel to receiver nodes located in the cells.

We first found the optimal configuration of the CellEVAC heuristic function parameters that control the allocation of exit gates (colors) to cells. This heuristic function depends on distance, congestion, flow, and inertia attributes. The simulation–optimization process applied the Tabu-search algorithm to obtain the parameters that weigh the distance, congestion, and flow attributes. The inertia attribute controls the number of decision changes induced, configured manually to obtain a reasonable number of exit-choice decision changes. The goal was to minimize the evacuation time and variance of cumulative density at the exits.

One important contribution of our study has been to model the behavior of evacuees not wearing LED wristbands. Our general requirements were to consider exit-choice and target speed determination processes, modeling the influence of leaders in the decision-making processes. To formalize the adaptive exit-choice processes, we opted by the three-layered modeling architecture proposed by Haghani and Sarvi (2019b), with an eligibility mechanism to avoid unfeasible exit-choice changing, an exit-choice decision changing module based on a binary logit formula, and an exit-choice decision module based on a multinomial logit model. The exit-choice decision changing module has been extended to include a new parameter that accounts for the change in the indications generated by the leader agents. This model has been calibrated using existing simulation and experimental data (Haghani and Sarvi, 2019b; Haghani et al., 2020) to maintain the decision change ratio at a low value. The most critical module regarding exit-choice decisions, the exit-choice decision module, was calibrated with hypothetical-choice experiments, replicating emergency evacuations with real participants. Finally, the choice of speed was modeled by evaluating leaders' influence in the exit-choice changing and exit-choice decision modules.

We have investigated the evacuation efficiency as a function of different levels of influence of leaders on evacuees and different population sizes of leaders, considering evacuation time and measurement of congestion and risk. To estimate the intrinsic risk of the pedestrian crowd, we used the "crowd pressure" metric, defined as the local variance of velocity multiplied by the corresponding density calculated using the concept of Voronoi diagrams. We took a macroscopic approach in the evaluation process using pedestrian Macroscopic Fundamental Diagrams representing crowd pressure vs. density points. Based on the pMFDs, we introduced the safety value as an estimation of risk, calculated as the proportion of crowd pressure vs. density points below a crowd pressure threshold.

The evidence from this study suggests the following:

- The viability of cell-based evacuation management systems as effective leader-based adaptive guidance systems based on exit-choice indications.
- The capability of the behavior modeling proposed to capture decision-making processes related to imitation and following behaviors, capturing the influence of leader agents.
- We may modulate the trade-off between evacuation time and safety by dimensioning and training the evacuation staff adequately.

- By varying the target speed of the leader agents, we may balance the expected evacuation time against the intrinsic risk of the crowd.
- Improving safety and the number of decision changes comes at the cost of higher evacuation times.
- The proposed leader-based guidance system performs well even in evacuation scenarios with heterogeneous populations of followers with different following behavior patterns.
- Feasibility of our modeling methodology and simulation–optimization framework as a general modeling architecture in which different guidance system modeling alternatives could fit.
- This proposal has high potential due to its simplicity, with a human–machine interface that provides simple instructions and a deployment cost and complexity expected to be small.

Several extensions to this research are being considered. We investigate the influence of different imitation and evacuation speed profiles on evacuation performance when using the leader-based CellEVAC system. We are also studying whether we can improve safety and evacuation time simultaneously by dynamically controlling the leaders' speed.

CRediT authorship contribution statement

Miguel A. Lopez-Carmona: Conceptualization, Methodology, Software, Formal analysis, Investigation, Writing – original draft, Writing – review & editing, Supervision. **Alvaro Paricio Garcia:** Software, Validation, Formal analysis, Investigation.

References

Abdelghany, A., Abdelghany, K., Mahmassani, H., Alhalabi, W., 2014. Modeling framework for optimal evacuation of large-scale crowded pedestrian facilities. European J. Oper. Res. 237, 1105–1118. http://dx.doi.org/10.1016/j.ejor.2014.02.054.

Akhter, F., Khadivizand, S., Siddiquei, H.R., Alahi, M.E.E., Mukhopadhyay, S., 2019. IoT enabled intelligent sensor node for smart city: Pedestrian counting and ambient monitoring. Sensors 19 (3374), http://dx.doi.org/10.3390/s19153374.

Alvarez Lopez, Y., de Cos Gomez, M.E., Las-Heras Andres, F., 2017. A received signal strength RFID-based indoor location system. Sensors Actuators A 255, 118–133. http://dx.doi.org/10.1016/j.sna.2017.01.007.

Antonini, G., Bierlaire, M., Weber, M., 2006. Discrete choice models of pedestrian walking behavior. Transp. Res. B 40, 667–687. http://dx.doi.org/10.1016/j.trb.2005.09.006.

BBC news, 2012. Spain Halloween stampede kills three in Madrid. https://www.bbc.com/news/world-europe-20166315.

Ben-Akiva, M., Bierlaire, M., 1999. Discrete choice methods and their applications to short term travel decisions. In: Hall, R.W. (Ed.), In: Handbook of Transportation Science International Series in Operations Research & Management Science, Springer US, Boston, MA, pp. 5–33.

Bi, H., Gelenbe, E., 2019. A survey of algorithms and systems for evacuating people in confined spaces. Electronics 8 (711), http://dx.doi.org/10.3390/electronics8060711.

Bode, N.W.F., Codling, E.A., 2013. Human exit route choice in virtual crowd evacuations. Anim. Behav. 86, 347–358. http://dx.doi.org/10.1016/j.anbehav.2013.05.025.

Bode, N.W.F., Codling, E.A., 2019. Exploring determinants of pre-movement delays in a virtual crowd evacuation experiment. Fire Technology 55, 595–615. http://dx.doi.org/10.1007/s10694-018-0744-9.

Bode, N.W.F., Kemloh Wagoum, A.U., Codling, E.A., 2014. Human responses to multiple sources of directional information in virtual crowd evacuations. J. R. Soc. Interface 11, 20130904. http://dx.doi.org/10.1098/rsif.2013.0904.

Bode, N.W.F., Kemloh Wagoum, A.U., Codling, E.A., 2015. Information use by humans during dynamic route choice in virtual crowd evacuations. Royal Soc. Open Sci. 2, http://dx.doi.org/10.1098/rsos.140410.

Brunetti, A., Buongiorno, D., Trotta, G.F., Bevilacqua, V., 2018. Computer vision and deep learning techniques for pedestrian detection and tracking: A survey. Neurocomputing 300, 17–33. http://dx.doi.org/10.1016/j.neucom.2018.01.092.

Chen, Y.-L., Liu, D., Wang, S., Li, Y.-F., Zhang, X.-S., 2019. Self-powered smart active RFID tag integrated with wearable hybrid nanogenerator. Nano Energy 64, 103911. http://dx.doi.org/10.1016/j.nanoen.2019.103911.

Chen, L., Tang, T.-Q., Huang, H.-J., Song, Z., 2018. Elementary students' evacuation route choice in a classroom: A questionnaire-based method. Physica A 492, 1066–1074. http://dx.doi.org/10.1016/j.physa.2017.11.036.

Correa, A., Barcelo, M., Morell, A., Vicario, J.L., 2017. A review of pedestrian indoor positioning systems for mass market applications. Sensors 17 (1927), http://dx.doi.org/10.3390/s17081927.

Dambalmath, P., Muhamad, B., Eberhard, H., Löhner, R., 2016. Fundamental diagrams for specific very high density crowds. Proc. Pedestr. Evacuation Dyn. 6–11.

Duives, D.C., Mahmassani, H.S., 2012. Exit choice decisions during pedestrian evacuations of buildings. Transp. Res. Rec. 2316, 84–94. http://dx.doi.org/10.3141/2316-10.

Ehtamo, H., Heliövaara, S., Korhonen, T., Hostikka, S., 2010. Game theoretic best-response dynamics for evacuees' exit selection. Adv. Complex Syst. 13, 113–134. http://dx.doi.org/10.1142/S021952591000244X.

Feliciani, C., Murakami, H., Shimura, K., Nishinari, K., 2020. Efficiently informing crowds– Experiments and simulations on route choice and decision making in pedestrian crowds with wheelchair users. Transp. Res. C 114, 484–503. http://dx.doi.org/10.1016/j.trc.2020.02.019.

Feliciani, C., Nishinari, K., 2016. Empirical analysis of the lane formation process in bidirectional pedestrian flow. Phys. Rev. E 94.

Feliciani, C., Nishinari, K., 2018. Measurement of congestion and intrinsic risk in pedestrian crowds. Transp. Res. C 91, 124–155. http://dx.doi.org/10.1016/j.trc.2018.03.027.

Ferscha, A., Zia, K., 2010. LifeBelt: Crowd evacuation based on vibro-tactile guidance. IEEE Pervasive Comput. 9, 33–42. http://dx.doi.org/10.1109/MPRV.2010.83.

Figueira, G., Almada-Lobo, B., 2014. Hybrid simulation–optimization methods: A taxonomy and discussion. Simul. Model. Pract. Theory 46, 118–134. http://dx.doi.org/10.1016/j.simpat.2014.03.007.

Fridolf, K., Ronchi, E., Nilsson, D., Frantzich, H., 2013. Movement speed and exit choice in smoke-filled rail tunnels. Fire Saf. J. 59, 8–21. http://dx.doi.org/10.1016/j.firesaf.2013.03.007.

Fruin, J.J., 1987.

Geroliminis, N., Daganzo, C.F., 2008. Existence of urban-scale macroscopic fundamental diagrams: Some experimental findings. Transp. Res. B 42, 759–770.

Geroliminis, N., Sun, J., 2011. Properties of a well-defined macroscopic fundamental diagram for urban traffic. Transp. Res. B 45, 605–617.

Glover, Fred, 1997. Tabu Search. Kluwer Academic Publishers.

Guo, R.-Y., 2018. Potential-based dynamic pedestrian flow assignment. Transp. Res. C 91, 263–275. http://dx.doi.org/10.1016/j.trc.2018.04.011.

Haghani, M., 2020a. Empirical methods in pedestrian, crowd and evacuation dynamics: Part II. Field methods and controversial topics. Saf. Sci. 129, 104760. http://dx.doi.org/10.1016/j.ssci.2020.104760.
Haghani, M., 2020b. Optimising crowd evacuations: Mathematical, architectural and behavioural approaches. Saf. Sci. 128, 104745. http://dx.doi.org/10.1016/j.ssci.2020.104745.
Haghani, M., Cristiani, E., Bode, N.W.F., Boltes, M., Corbetta, A., 2019. Panic, irrationality, and herding: Three ambiguous terms in crowd dynamics research. J. Adv. Transp. 2019, e9267643. http://dx.doi.org/10.1155/2019/9267643.
Haghani, M., Ejtemai, O., Sarvi, M., Sobhani, A., Burd, M., Aghabayk, K., 2014. Random utility models of pedestrian crowd exit selection based on SP-off-RP experiments. Transp. Res. Proc. 2, 524–532. http://dx.doi.org/10.1016/j.trpro.2014.09.070.
Haghani, M., Sarvi, M., 2017. Stated and revealed exit choices of pedestrian crowd evacuees. Transp. Res. B 95, 238–259.
Haghani, M., Sarvi, M., 2018. Crowd behaviour and motion: Empirical methods. Transp. Res. B 107, 253–294.
Haghani, M., Sarvi, M., 2019a. Heterogeneity of decision strategy in collective escape of human crowds: On identifying the optimum composition. Int. J. Disaster Risk Reduct. 35, 101064. http://dx.doi.org/10.1016/j.ijdrr.2019.101064.
Haghani, M., Sarvi, M., 2019b. Simulating dynamics of adaptive exit-choice changing in crowd evacuations: Model implementation and behavioural interpretations. Transp. Res. C 103, 56–82. http://dx.doi.org/10.1016/j.trc.2019.04.009.
Haghani, M., Sarvi, M., Shahhoseini, Z., 2015. Accommodating taste heterogeneity and desired substitution pattern in exit choices of pedestrian crowd evacuees using a mixed nested logit model. J. Choice Model. 16, 58–68.
Haghani, M., Sarvi, M., Shahhoseini, Z., 2020. Evacuation behaviour of crowds under high and low levels of urgency: Experiments of reaction time, exit choice and exit-choice adaptation. Saf. Sci. 126, 104679. http://dx.doi.org/10.1016/j.ssci.2020.104679.
Haghani, M., Sarvi, M., Shahhoseini, Z., Boltes, M., 2016. How simple hypothetical-choice experiments can be utilized to learn humans' navigational escape decisions in emergencies. PLOS ONE 11, e0166908. http://dx.doi.org/10.1371/journal.pone.0166908.
Helbing, D., Johansson, A., Al-Abideen, H.Z., 2007. Dynamics of crowd disasters: An empirical study. Phys. Rev. E 75.
Helbing, D., Molnár, P., 1995. Social force model for pedestrian dynamics. Phys. Rev. E 51, 4282–4286. http://dx.doi.org/10.1103/PhysRevE.51.4282.
Helbing, D., Mukerji, P., 2012. Crowd disasters as systemic failures: Analysis of the love parade disaster. EPJ Data Sci. 1, 1–40.
Hoogendoorn, S.P., Bovy, P.H.L., 2004. Pedestrian route-choice and activity scheduling theory and models. Transp. Res. B 38, 169–190. http://dx.doi.org/10.1016/S0191-2615(03)00007-9.
Hoogendoorn, S.P., Daamen, W., Knoop, V.L., Steenbakkers, J., Sarvi, M., 2018. Macroscopic fundamental diagram for pedestrian networks: Theory and applications. Transp. Res. C 94, 172–184.
Hoogendoorn, S.P., Daamen, W., Knoop, V.L., Steenbakkers, J., Sarvi, M., 2018b. Macroscopic fundamental diagram for pedestrian networks: Theory and applications. Transp. Res. C 94, 172–184. http://dx.doi.org/10.1016/j.trc.2017.09.003.
Ilyas, N., Shahzad, A., Kim, K., 2020. Convolutional-neural network-based image crowd counting: Review, categorization, analysis, and performance evaluation. Sensors 20 (43), http://dx.doi.org/10.3390/s20010043.
Jacques, J.C.S., Mussef, S.R., Jung, C.R., 2010. Crowd analysis using computer vision techniques. IEEE Signal Process. Mag. 27, 66–77.
Johansson, A., Helbing, D., Al-Abideen, H.Z., Al-Bosta, S., 2008. From crowd dynamics to crowd safety: A video-based analysis. Adv. Complex Syst. 11, 497–527.
Kaiser, M.S., Lwin, K.T., Mahmud, M., Hajializadeh, D., Chaipimonplin, T., Sarhan, A., Hossain, M.A., 2018. Advances in crowd analysis for urban applications through urban event detection. IEEE Trans. Intell. Transp. Syst. 19, 3092–3112. http://dx.doi.org/10.1109/TITS.2017.2771746.
Kinateder, M., Comunale, B., Warren, W.H., 2018. Exit choice in an emergency evacuation scenario is influenced by exit familiarity and neighbor behavior. Saf. Sci. 106, 170–175. http://dx.doi.org/10.1016/j.ssci.2018.03.015.
Kneidl, A., Hartmann, D., Borrmann, A., 2013. A hybrid multi-scale approach for simulation of pedestrian dynamics. Transp. Res. C 37, 223–237. http://dx.doi.org/10.1016/j.trc.2013.03.005.
Kok, V.J., Lim, M.K., Chan, C.S., 2016. Crowd behavior analysis: A review where physics meets biology. Neurocomputing 177, 342–362. http://dx.doi.org/10.1016/j.neucom.2015.11.021.
Kurkcu, A., Ozbay, K., 2017. Estimating pedestrian densities, wait times, and flows with wi-fi and bluetooth sensors. Transp. Res. Rec. 2644, 72–82. http://dx.doi.org/10.3141/2644-09.
Lesani, A., Nateghinia, E., Miranda-Moreno, L.F., 2020. Development and evaluation of a real-time pedestrian counting system for high-volume conditions based on 2D lidar. Transp. Res. C 114, 20–35. http://dx.doi.org/10.1016/j.trc.2020.01.018.
Lopez-Carmona, M.A., Paricio-Garcia, A., 2020. LED wristbands for cell-based crowd evacuation: An adaptive exit-choice guidance system architecture. Sensors 20 (6038), http://dx.doi.org/10.3390/s20216038.
Lopez-Carmona, M.A., Paricio Garcia, A., 2021. CellEVAC: An adaptive guidance system for crowd evacuation through behavioral optimization. Saf. Sci. 139, 105215. http://dx.doi.org/10.1016/j.ssci.2021.105215.
Lovreglio, R., Borri, D., dell'Olio, L., Ibeas, A., 2014. A discrete choice model based on random utilities for exit choice in emergency evacuations. Saf. Sci. 62, 418–426. http://dx.doi.org/10.1016/j.ssci.2013.10.004.
Lu, L., Chan, C.-Y., Wang, J., Wang, W., 2017. A study of pedestrian group behaviors in crowd evacuation based on an extended floor field cellular automaton model. Transp. Res. C 81, 317–329. http://dx.doi.org/10.1016/j.trc.2016.08.018.
Luce, R.D., 1958. A probabilistic theory of utility. Econometrica 26, 193–224. http://dx.doi.org/10.2307/1907587.
Mao, Y., Fan, X., Fan, Z., He, W., 2019. Modeling group structures with emotion in crowd evacuation. IEEE Access 7, 140010–140021. http://dx.doi.org/10.1109/ACCESS.2019.2943603.
Molloy, J., Becker, F., Schmid, B., Axhausen, K.W., 2021. Mixl: An open-source R package for estimating complex choice models on large datasets. J. Choice Model. 39, 100284. http://dx.doi.org/10.1016/j.jocm.2021.100284.
Murakami, H., Feliciani, C., Shimura, K., Nishinari, K., 2020. A system for efficient egress scheduling during mass events and small-scale experimental demonstration. Royal Soc. Open Sci. 7, 201465. http://dx.doi.org/10.1098/rsos.201465.
Nguyen-Huu, K., Lee, K., Lee, S.-W., 2017. An indoor positioning system using pedestrian dead reckoning with WiFi and map-matching aided. In: 2017 International Conference on Indoor Positioning and Indoor Navigation (IPIN). pp. 1–8. http://dx.doi.org/10.1109/IPIN.2017.8115898.
Ortúzar, J., Willumsen, L., 2011. Modelling Transport, fourth ed. John Wiley and Sons, New York.
Press, T.M., 1985. Discrete choice analysis. https://mitpress.mit.edu/books/discrete-choice-analysis.
Saberi, M., Mahmassani, H.S., 2014. Exploring areawide dynamics of pedestrian crowds: Three-dimensional approach. Transp. Res. Rec. 2421, 31–40. http://dx.doi.org/10.3141/2421-04.
Steffen, B., Seyfried, A., 2010. Methods for measuring pedestrian density, flow, speed and direction with minimal scatter. Physica A 389, 1902–1910.
Tianhe, J., Ziheng, S., 2018. Optimal control on crowd evacuation with leader-follower model. In: 2018 11th International Symposium on Computational Intelligence and Design (ISCID). Vol. 02, pp. 236–239. http://dx.doi.org/10.1109/ISCID.2018.10155.
Train, K., 2009. Discrete Choice Methods with Simulation. Cambridge University Press.
Truong, L.T., Nguyen, H.T.T., Nguyen, H.D., Vu, H.V., 2019. Pedestrian overpass use and its relationships with digital and social distractions, and overpass characteristics. Accid. Anal. Prev. 131, 234–238. http://dx.doi.org/10.1016/j.aap.2019.07.004.
Wang, H.-R., Chen, Q.-G., Yan, J.-B., Yuan, Z., Liang, D., 2015. Emergency guidance evacuation in fire scene based on pathfinder. In: Proceedings - 7th International Conference on Intelligent Computation Technology and Automation, ICICTA 2014. pp. 226–230. http://dx.doi.org/10.1109/ICICTA.2014.62.

Xie, W., Lee, E.W.M., Li, T., Shi, M., Cao, R., Zhang, Y., 2021. A study of group effects in pedestrian crowd evacuation: Experiments, modelling and simulation. Saf. Sci. 133, 105029. http://dx.doi.org/10.1016/j.ssci.2020.105029.

Zhang, Z., Jia, L., 2021. Optimal guidance strategy for crowd evacuation with multiple exits: A hybrid multiscale modeling approach. Appl. Math. Model. 90, 488–504. http://dx.doi.org/10.1016/j.apm.2020.08.075.

Zhang, J., Seyfried, A., 2013. Empirical characteristics of different types of pedestrian streams. Procedia Eng. 62, 655–662. http://dx.doi.org/10.1016/j.proeng.2013.08.111.

Zhang, X.L., Weng, W.G., Yuan, H.Y., 2012. Empirical study of crowd behavior during a real mass event. J. Stat. Mech. Theory Exp. P08012. http://dx.doi.org/10.1088/1742-5468/2012/08/P08012.

Zhong, J., Cai, W., Luo, L., 2016. Crowd evacuation planning using Cartesian Genetic Programming and agent-based crowd modeling. In: Volume 2016-February of Proceedings - Winter Simulation Conference. pp. 127–138. http://dx.doi.org/10.1109/WSC.2015.7408158.

Zhong, J., Ong, Y.-S., Cai, W., 2016b. Self-learning gene expression programming. IEEE Trans. Evol. Comput. 20, 65–80. http://dx.doi.org/10.1109/TEVC.2015.2424410.

Zhou, M., Dong, H., Ioannou, P.A., Zhao, Y., Wang, F., 2019a. Guided crowd evacuation: Approaches and challenges. IEEE/CAA J. Autom. Sin. 6, 1081–1094. http://dx.doi.org/10.1109/JAS.2019.1911672.

Zhou, M., Dong, H., Zhao, Y., Ioannou, P.A., Wang, F.-Y., 2019b. Optimization of crowd evacuation with leaders in urban rail transit stations. IEEE Trans. Intell. Transp. Syst. 20, 4476–4487. http://dx.doi.org/10.1109/TITS.2018.2886415.